การวิเคราะห์ทางอุณหพลศาสตร์ของการผลิตไฮโดรเจนจากกลีเซอรอล

ด้วยกระบวนการรีฟอร์มมิ่งที่ต่างกัน

นางสาว กิรณา จิรโชติเดโช

THERMODYNAMIC ANALYSIS OF HYDROGEN PRODUCTION FROM
GLYCEROL WITH DIFFERENT REFORMING PROCESSES

Miss Ghirana Jirachotdaecho

A Thesis Submitted in Partial Fulfillment of the Requirements

for the Degree of Master Engineering Program in Chemical Engineering

Department of Chemical Engineering

Faculty of Engineering
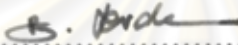
Chulalongkorn University

Academic Year 2009

Thesis Title	THERMODYNAMIC ANALYSIS OF HYDROGEN
	PRODUCTION FROM GLYCEROL WITH
	DIFFERENT REFORMING PROCESSES
By	Miss Ghirana Jirachotdaecho
Field of Study	Chemical Engineering
Thesis Advisor	Assistant Professor Amornchai Arpornwichanop, D.Eng.

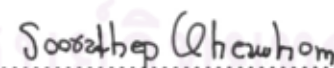
Accepted by the Faculty of Engineering, Chulalongkorn University in Partial Fulfillment of the Requirements for the Master's Degree

.... Dean of the Faculty of Engineering

(Associate Professor Boonsom Lerdhirunwong, Dr.Ing.)

THESIS COMMITTEE

.... Chairman

(Associate Professor Muenduen Phisalaphong, Ph.D.)

.... Thesis Advisor

(Assistant Professor Amornchai Arpornwichanop, D.Eng.)

.... Examiner

(Assistant Professor Soorathep Kheawhom, Ph.D.)

.... External Examiner

(Woranee Paengjuntuek, D.Eng.)

กิรณา จิรโชติเดโช: การวิเคราะห์ทางอุณหพลศาสตร์ของการผลิตไฮโดรเจนจาก
กลีเซอรอลด้วยกระบวนการรีฟอร์มมิ่งที่ต่างกัน. (THERMODYNAMIC ANALYSIS
OF HYDROGEN PRODUCTION FROM GLYCEROL WITH DIFFERENT
REFORMING PROCESSES) อ.ที่ปรึกษาวิทยานิพนธ์หลัก : ผศ.ดร. อมรชัย
อาภรณ์วิชานพ, 79 หน้า.

งานวิจัยนี้ทำการวิเคราะห์เชิงอุณหพลศาสตร์ของกระบวนการผลิตไฮโดรเจนจาก
กลีเซอรอลซึ่งเป็นผลพลอยได้จากการผลิตไบโอดีเซล ด้วยกระบวนการรีฟอร์มมิ่งที่แตกต่างกัน
ดังนี้ กระบวนการรีฟอร์มมิ่งด้วยไอน้ำ กระบวนการออกซิเดชั่นบางส่วน และกระบวนการ
ออโตเทอร์มอลรีฟอร์มมิ่ง การศึกษาโดยการจำลองเพื่อหาผลของพารามิเตอร์ที่เกี่ยวข้องกับการ
ดำเนินงาน ได้แก่ อุณหภูมิการเกิดปฏิกิริยา อัตราส่วนของไอน้ำกับกลีเซอรอล และ อัตราส่วน
ของออกซิเจนกับกลีเซอรอล ที่มีต่อสมรรถนะเครื่องปฏิกรณ์รีฟอร์มเมอร์ในแง่การผลิต
ไฮโดรเจนและความต้องการพลังงานความร้อน ผลที่ได้แสดงให้เห็นว่าผลกระทบจากปฏิกิริยา
การเกิดมีเทน ทำให้ไฮโดรเจนที่ผลิตได้ลดลง เมื่อเพิ่มอัตราส่วนเชิงโมลของไอน้ำต่อกลีเซอรอล
ปริมาณไฮโดรเจนที่ได้และความต้องการพลังงานความร้อนของกระบวนการรีฟอร์มมิ่งด้วยไอน้ำ
จะเพิ่มขึ้น ขณะที่ปริมาณไฮโดรเจนจะลดลงเมื่อเพิ่มอัตราส่วนเชิงโมลของออกซิเจนต่อ
กลีเซอรอลในกระบวนการออกซิเดชั่นบางส่วน สำหรับกระบวนการออโตเทอร์มอลรีฟอร์มมิ่ง
นั้น พบว่าจะเกิดปฏิกิริยารีฟอร์มมิ่งด้วยไอน้ำได้ดีกว่าปฏิกิริยาออกซิเดชั่นบางส่วน ที่อุณหภูมิสูง
ปฏิกิริยารีเวอร์สวอเตอร์แก๊สชิฟ (reverse water gas shift) เป็นปฏิกิริยาหลักที่เกิดขึ้น เมื่อทำการ
เปรียบเทียบระหว่างกระบวนการรีฟอร์มมิ่งที่ต่างกัน กระบวนการรีฟอร์มมิ่งด้วยไอน้ำสามารถ
ผลิตไฮโดรเจนได้มากที่สุด รองลงมาคือกระบวนการออโตเทอร์มอลรีฟอร์มมิ่ง และกระบวนการ
ออกซิเดชั่นบางส่วน อย่างไรก็ตามเมื่อพิจารณาความต้องการพลังงานโดยรวม กระบวนการ
รีฟอร์มมิ่งด้วยไอน้ำต้องการพลังงานความร้อนมากที่สุด รองลงมาคือกระบวนการออโต
เทอร์มอลรีฟอร์มมิ่ง

ภาควิชา	วิศวกรรมเคมี	ลายมือชื่อนิสิต	กิรณา จิรโชติเดโช
สาขาวิชา	วิศวกรรมเคมี	ลายมือชื่อ อ.ที่ปรึกษาวิทยานิพนธ์หลัก	
ปีการศึกษา	2552		

5070222921   : MAJOR CHEMICAL ENGINEERING

KEYWORDS : HYDROGEN PRODUCTION / GLYCEROL / REFORMING / PARTIAL OXIDATION / AUTOTHERMAL REFORMING

GHIRANA JIRACHOTDAECHO: THERMODYNAMIC ANALYSIS OF HYDROGEN PRODUCTION FROM GLYCEROL WITH DIFFERENT REFORMING PROCESSES. THESIS ADVISOR: ASST.PROF. AMORNCHAI ARPORNWICHANOP, D.Eng., 79 pp.

In this study, a thermodynamic analysis of hydrogen production from glycerol, a by-product of biodiesel production, using different reforming processes, i.e., steam reforming, partial oxidation and autothermal reforming, was investigated. Simulation studies were performed to determine the influence of key operating parameters, i.e., reaction temperature, steam-to-glycerol (S/G) molar feed ratio, and oxygen-to-glycerol (O/G) molar feed ratio, on the performance of a reformer in terms of hydrogen production and heat requirement. The results show that the effect of a side reaction of methanation leads to a decrease in hydrogen production. When a molar feed ratio of S/G increases, the yield of hydrogen and energy demand of the steam reforming process increases. The hydrogen yield also increases with increasing the O/G molar ratio in the partial oxidation process in which the O/G ratio also affects a total heat demand. For the autothermal reforming, it is found that the partial oxidation reaction is more pronounced than the steam reforming reaction. At high temperature, the reverse water gas shift is the dominant reaction. Comparing among different reforming options, the steaming reforming process can produce the highest amount of hydrogen, followed by the autothermal reforming and the partial oxidation processes. However, when considering the total energy demand, the steam reforming is the most requiring energy supply, followed by autothermal reforming process.

Department :   Chemical Engineering   Student's Signature : Ghirana   Jirachotdaecho

Field of Study :   Chemical Engineering   Advisor's Signature : Amornchai Arpornwichanop

Academic Year : _2009_

ACKHOWLEDGEMENTS

CONTENTS

LIST OF TABLES

LIST OF FIGURES

NOMENCLATURES

ATR	Autothermal reforming
POX	Partial oxidation
R_{pox}	Oxygen-to-glycerol molar ratio
R_{sr}	Water-to-glycerol molar ratio
R-WGS	Reverse water gas shift
SR	Steam reforming
WGS	Water gas shift
G	Gibbs free energy
ξ	The extent of reaction
T	Absolute temperature
p	Absolute pressure
μ_i	A partial molar Gibbs energy for component i
R	Ideal gas constant (8.314472 J/(mole K))
Q_r	The reaction quotient
K_{eq}	The equilibrium constant

CHAPTER I

INTRODUCTION

1.1 Motivation

Hydrogen is considered as one of the most promising energy carriers that would replace to use of the fossil fuel in the future. Besides its direct uses as the automotive fuel, hydrogen can be efficiently converted into many useful energy forms. One of the most attractive hydrogen technologies is fuel cell, an electrochemical devices that converting the chemical energy of a fuel into electricity. However, a major obstacle for hydrogen energy system is a lack of hydrogen supply in the energy carrier form. In general, hydrogen can be prepared by different methods and from various sources. A reforming process is the most widely used technology for hydrogen production. Among the various types of petroleum-derived fuels, i.e., methane, methanol, ethanol and glycerol, methane as the major component of natural gas which is a convenient feedstock because the existing natural gas pipeline infrastructure makes it readily available and accessible at any point along the distributed chain.

Presently, the depletion of petroleum feedstock and the awareness of environmental impact have motivated researchers to explore an alternative resource and a novel technology to produce hydrogen efficiently. Biomass has received considerable attention as an attractive energy source because it is renewable and, theoretically, carbon dioxide neutral. Recently, biodiesel, an alternative to petroleum diesel, is considered as a good example of using biomass to produce alternative energy. The use of biodiesel and its production are expected to grow in the future. With increased production of biodiesel, glycerol as a by-product is expected in the world market and therefore it is essential to find useful applications for glycerol. Glycerol can be used in many applications including food, personal care, oral care, polymer and pharmaceutical applications. Several commercial plants have been established recently to produce propylene glycol from glycerol.

Producing hydrogen from glycerol is another interesting approach. To date only a few studies have been attempted on glycerol reforming for hydrogen production. The current industrial process involves the steam reforming because it is well-established

technology. However, other alternative routes, i.e., partial oxidation whish is an exothermic process and autothermal reforming combined with steam reforming and partial oxidation, should be considered. Reforming of glycerol for hydrogen production involves complex reactions. As a result, several intermediate byproducts are formed and end up in the product stream affecting the final purity of hydrogen produced. Furthermore, the yield of the hydrogen depends on several process variables, such as the operating temperature, water-to-glycerol molar feed ratio and oxygen-to-glycerol molar feed ratio. The first step to understanding the effects of the aforementioned variables is a complete thermodynamic analysis and then varies the operating parameters. From this study, ideal reaction conditions for the reforming process, steam reforming, partial oxidation and autothermal reforming, of glycerol to produce maximize hydrogen yield and minimize undesirable products can be determined.

1.2 Objectives

To analyze the effects of operating parameters on the production of hydrogen from glycerol using different reforming processes, i.e., steam reforming, partial oxidation, and autothermal reforming processes.

To define the optimal operating conditions of the different glycerol reforming processes for obtaining the best overall efficiency.

1.3 Scopes of work

In this study, a glycerol reforming process for hydrogen production is investigated. The glycerol reforming process consisting of an evaporator, a reformer and a water gas shift reactor is simulated by using HYSYS 3.1 simulator. The effects of various operating parameters, i.e., feed preheating temperature, reaction temperature, and molar feed ratio such as steam to glycerol (S/G) ratio and oxygen to glycerol (O/G) ratio on the production of hydrogen is presented. The heat integration of glycerol reforming processes is also considered. And then compare the performance of each process.

CHAPTER II

THEORY

The renewable energy sources i.e. wind, solar, ocean, and biomass will be the most important source for the production of hydrogen. Because regenerative hydrogen, hydrogen produced from nuclear sources and fossil-based energy conversion systems with capture, and safe storage (sequestration) of CO_2 emissions, are almost completely carbon-free energy pathways, the renewable energy sources become more widely available (Fig. 2.1).

2.1 Hydrogen production

Hydrogen is a clean energy resource as only steam is generated during a combustion process.

$$2H_2 + O_2 \rightarrow 2H_2O \qquad \Delta H_{298K} = -482 \ kJ/mol \qquad (2.1)$$

Presently, hydrogen is produced almost entirely from petroleum-based fuels such as natural gas, gasoline, naphtha, and coal. In such cases, however, the same amount of carbon dioxide is released during the production of hydrogen as that formed by direct combustion of those fuels. Due to the depletion of fossil fuels, the use of alternative resources such as renewable biomass gains significant research interest. Biomass, an organic material made from plants and animals, is a renewable energy source because it can always grow more trees and crops, and waste will always exist. Burning of biomass is released heat and usable forms of energy like methane gas or transportation fuels like ethanol and biodiesel. Moreover, wood waste or garbage can be burned to produce steam for making electricity, or to provide heat to industries and homes. Biomass does not release pollutants like sulfur, which can cause acid rain when it is burned. Biomass only releases carbon dioxide, a greenhouse gas. But when biomass crops are grown, a nearly equivalent amount of carbon dioxide is captured through photosynthesis.
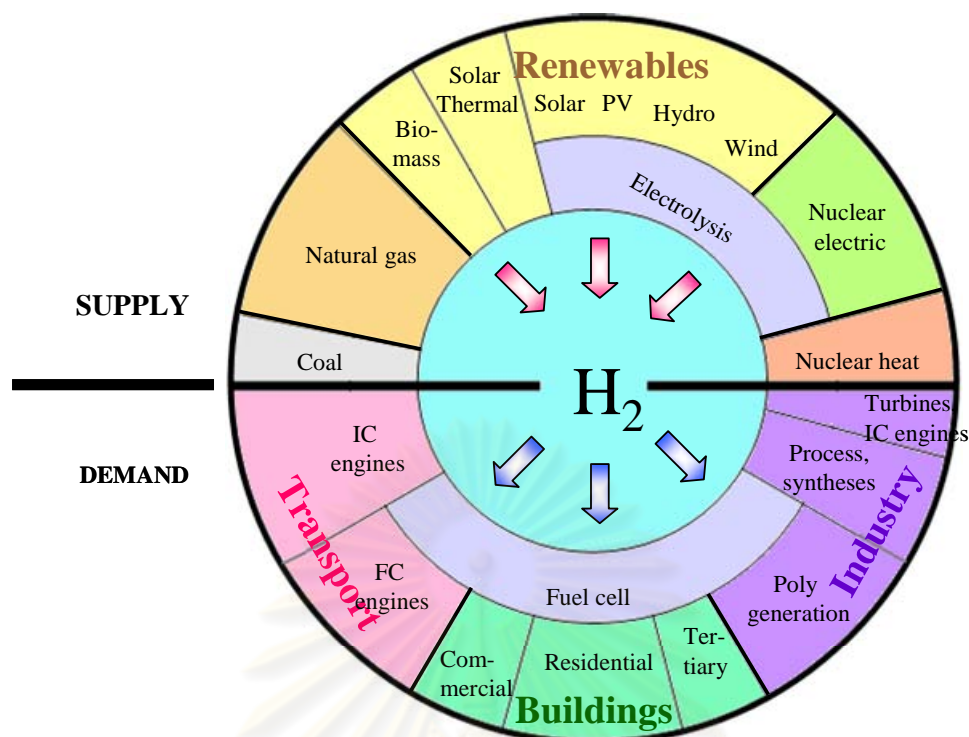
Fig. 2.1 Hydrogen: primary energy sources, energy converters and applications (Rodriguez G., 2006)

Biofuels, usually blended with the petroleum fuels - gasoline and diesel fuel, are made from biomass materials. The biodiesel is a renewable fuel that can be used instead of diesel fuel made from petroleum. Because it is so clean burning and easy to use, biodiesel is the fastest growing and most cost efficient fuel for fleet vehicles. Biodiesel is most often blended with petroleum diesel in ratios of 2 percent (B_2), 5 percent (B_5), and 20 percent (B_{20}). It can also be used as pure biodiesel (B_{100}). Biodiesel fuels can be used in regular diesel vehicles without making any changes to the engines. It can also be stored and transported using diesel tanks and equipment.

Glycerol, by-product obtained from bio-diesel plants, can be effectively applied for hydrogen production by transesterification process of vegetable oils (triglycerides) and methanol. The process of transesterification is affected by the reaction conditions, molar ratio of alcohol to oil, type of alcohol used, type and amount of catalysts employed, reaction time, temperature and the purity of the reagents. Given the forecasted increases in biodiesel production, the by-production, glycerol – the unique character of being non-toxic, non-volatile and non-flammable, is predicted to increase markedly in the near future. Technical grade crude glycerol (85-88% dry matter) is a yellowish brown, viscous liquid with a sweet taste. Using in pharmaceutical, the crude product must be purified to

99.5 %. The utilization of glycerol to produce hydrogen or synthesis gas could potentially reduce the production costs of biodiesel. Synthesis gas is of great importance as a major chemical intermediate in chemical processes for the synthesis of several fuels and chemicals.

2.2 Hydrogen production processes

In general, hydrogen can be produced from several routes, i.e., reforming process, pyrolysis, gasification and electrolysis of water. Many profits of any processes are shown in this part.

2.2.1 Reforming process

The reforming process including steam reforming, partial oxidation and autothermal reforming can be convert hydrocarbon into hydrogen or synthesis gas. From Fig. 2.2, hydrocarbons pass though the reforming reactor. Then, let the hydrogen and/or synthesis gas produced from the reformer to purify and separate to pure component.
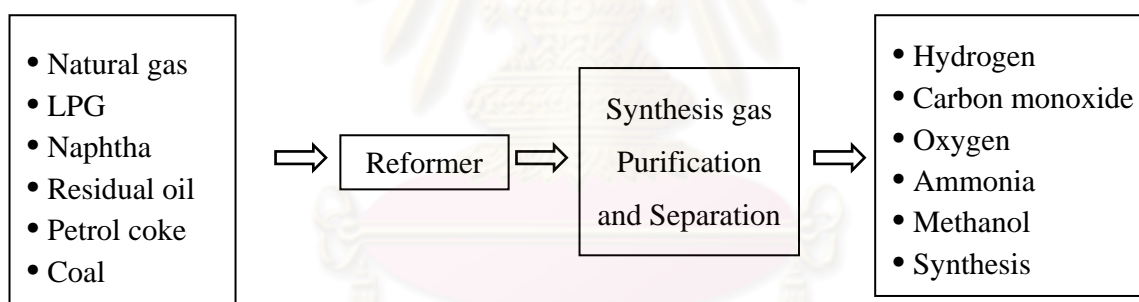
Fig. 2.2 The stepwise of reformer process for hydrogen production

Steam reforming

Steam reforming (SR) is one of the widely used methods which convert hydrocarbons with steam into a mixture of hydrogen and carbon monoxide, also known as synthesis gas (syngas). This process is highly endothermic so that it needs to have a lot of heat from external sources. It is usually operated at temperatures less than 800 $^{\circ}$C in order to avoid the deactivation and thermal sintering of the catalyst and the regeneration of reformer on Ni-based catalyst. However, a small-scale steam reforming unit is currently subject to scientific researches and generally the most economic way to produce hydrogen to fuel cells for automobile applications. Today, steam reforming of natural gas is widely used in industry.

Partial Oxidation

A partial oxidation (POX) is one of the important processes for the hydrogen production. This process occurs when a fuel and air mixture at a sub-stoichiometric ratio is partially combusted in a reformer. The advantage of partial oxidation over steam reforming of the fuel is that it is an exothermic reaction rather than an endothermic reaction and therefore generates its own heat; the outlet temperature is higher than 1500 ^{o}C. Due to high temperature operation, the cost of reactor materials are rising and soot can easily emerge. The catalytic partial oxidation process has captured wide attention as a noteworthy method that can reduce production costs in the future.

Autothermal reforming

Autothermal reforming (ATR) is the combination of two processes of steam reforming and partial oxidation, in order to achieve a minimum energy input necessary to maintain the required reformer temperature. It offers advantages of small unit size and lower operational temperature, easier startup, and wider choice of materials. Moreover, compared to other reforming processes, ATR has low energy requirements and can easily regulate the H_2/CO ratio of product stream by changing inlet gas composition. Although ATR has an interesting potential in industrial applications, there has been only a limited number of work reported in the field of reactor design and simulation.

2.2.2 Pyrolysis

Pyrolysis is the chemical decomposition of a condensed substance by heating so that it often occurs spontaneously at high temperatures. Furthermore, it does not involve reactions with oxygen or any other reagents but can take place in their presence. It is a special case of thermolysis and most commonly used for organic materials. This process leaves only carbon called carbonization as the residue and is related to the chemical process of charring. Pyrolysis is heavily used in the chemical industry, for example, to produce charcoal, activated carbon, methanol and other chemicals from wood, to convert ethylene dichloride into vinyl chloride to make PVC, to produce coke from coal, to convert biomass into synthesis gas, to turn waste into safely disposable substances, and for the cracking of medium-weight hydrocarbons from oil to produce lighter ones like gasoline.

2.2.3 Gasification

The gasification is a process that converts hydrocarbon such as coal, petroleum, or biomass into carbon monoxide and hydrogen by reacting the raw material at high temperatures with a controlled amount of oxygen and/or steam. Gasification is a very significant method for extracting energy from many different types of organic materials and also has applications as a clean waste disposal technique. The process relies on chemical processes at elevated temperatures (>700 °C), which distinguishes it from biological processes such as anaerobic digestion that produce biogas. The advantage of gasification is that using the syngas produced is potentially more efficient than direct combustion of the original fuel because it can be combusted at higher temperatures or even in fuel cells.

2.2.4 Electrolysis of water

Electrolysis is the decomposition of water (H_2O) into oxygen (O_2) and hydrogen (H_2) due to an electric current being passed through the water. This electrolytic process is used in some industrial applications when hydrogen is needed. An electrical power source is connected to two electrodes or two plates (typically made from some inert metal such as platinum or stainless steel) which are placed in the water. Hydrogen will appear at the cathode (the negatively charged electrode, where electrons are pumped into the water), and oxygen will appear at the anode (the positively charged electrode). The generated amount of hydrogen is twice the amount of oxygen, and both are proportional to the total electrical charge that was sent through the water.

2.2.5 Biological production

Biological hydrogen production has several advantages over hydrogen production by photoelectrochemical or thermochemical processes. Biological hydrogen production by photosynthetic microorganisms for example, requires the use of a simple solar reactor such as a transparent closed box, with low energy requirements. Biological hydrogen production processes are found to be more environment friendly and less energy intensive as compared to thermochemical and photoelectrochemical processes. Genetic manipulation of cyanobacteria (hydrogenase negative gene) uses to improve the hydrogen generation.

Table 2.1 Summary of hydrogen production technologies

Hydrogen production technology	Benefits	Barriers
Reforming: Splitting of hydrocarbon fuel with heat and steam	- Low- cost to produce hydrogen from natural gas - Well-understood at large scale and widespread - Opportunity to combine with large scale CO_2 sequestration (carbon storage)	- Small-scale units not commercial - Hydrogen contains some impurities - CO_2 emissions - Primary fuel may be used directly
Pyrolysis: Chemically decomposes of organic materials by heat in the absence of oxygen	- Treat and destroy semi-volatile organic compounds, fuels and pesticides in soil	– Products creation of incomplete combustion, including dioxins and furans which are extremely toxic in the parts per trillion range - The molten salt is usually recycled in the reactor chamber - May be removing volatile metals but not destroyed - Requiring proper treatment, storage and disposal for oils and tars (hazardous wastes)

Table 2.1 Summary of hydrogen production technologies (continue)

Gasification: Splitting heavy hydrocarbons and biomass into hydrogen and gases for reforming	- Well-understood for heavy hydrocarbons at large scale - It can be used for solid and liquid fuels - Possible synergies with synthetic fuels from biomass gasification being demonstrated	- Small units very rare - Hydrogen usually requires extensive cleaning before use - Biomass gasification still under research - Biomass has land-use implications - Competition with synthetic fuels from biomass
Electrolysis: Splitting water by using electricity	- Commercially available with proven technology - Well-understood industrial process - High purity hydrogen, convenient for producing hydrogen from renewable electricity	- Competition with direct use of renewable electricity
Biological production: Algae and bacteria produce hydrogen directly in some conditions	- Potentially large resource	- Slow hydrogen production rates - Large area needed - Most appropriate organisms not yet found - Still under research

2.3 Use of Glycerol for hydrogen production

Due to decease in petroleum reserves and an increase in environmental concerns, alternative energy resources are becoming increasingly important. On the other hand, demand for hydrogen (H_2) is growing due to the technological advancements in the fuel cell industry. Hydrogen can be produced from biobased resources via steam reforming, gasification, and pyrolysis. With ever-increasing production of biodiesel, an inexpensive

glycerol has resulted in the world market. Several alternatives are being explored to utilize glycerol, a byproduct from biodiesel plants. For example, several commercial plants have been established recently to produce propylene glycol from glycerol. Producing H_2 from glycerol is another approach that is being investigated in this work.

Glycerol is able to be converted into synthesis gas, a mixture of hydrogen and carbon monoxide, via several catalytic reactions including steam reforming, partial oxidation, and autothermal reforming.

Glycerol steam reforming

Steam reforming, is the established process for converting steam and lighter hydrocarbon such as natural gas or refinery feedstock into synthesis gas. In the reforming process of alcohol, such as glycerol, many reactions are likely to occur. The reaction which is the ideality pathway for the highest hydrogen is shown as

$$C_3H_8O_3 + 3H_2O \Leftrightarrow 3CO_2 + 7H_2 \qquad \Delta H_{298K} = +127.67 \ \text{kJ/mol} \qquad (2.2)$$
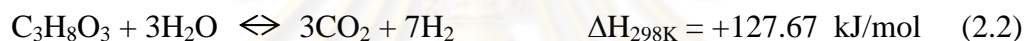
Partial oxidation of glycerol

Glycerol can also be converted to hydrogen-rich gas via an exothermic partial oxidation process. The general reaction is described by

$$C_3H_8O_3 + \frac{1}{2}O_2 \Leftrightarrow 2CO + CO_2 + 4H_2 \qquad \Delta H_{298K} = -31.79 \ \text{kJ/mol} \qquad (2.3)$$

$$C_3H_8O_3 + O_2 \Leftrightarrow CO + 2CO_2 + 4H_2 \qquad \Delta H_{298K} = -314.76 \ \text{kJ/mol} \qquad (2.4)$$

$$C_3H_8O_3 + \frac{3}{2}O_2 \Leftrightarrow 3CO_2 + 4H_2 \qquad \Delta H_{298K} = -597.73 \ \text{kJ/mol} \qquad (2.5)$$

$$C_3H_8O_3 + \frac{7}{2}O_2 \Leftrightarrow 3CO_2 + 4H_2 \qquad \Delta H_{298K} = -1564.93 \ \text{kJ/mol} \qquad (2.6)$$
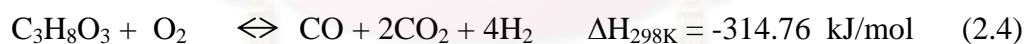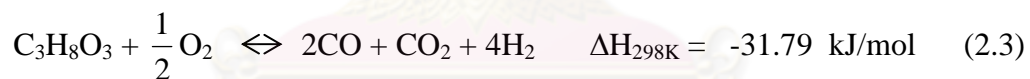
In this work, the only Eq. 2.5 is used in the process because H_2O and CO limiting in fuel cell is occurred in other Equation.

It is noted that from Eqs. 2.2 and 2.5, both the reactions has carbon dioxide as a by-product which can be used to produce carbon monoxide by the reverse water gas shift reaction.

2.4 Reverse water gas shift reaction

The reverse water gas shift reaction is an endothermic process and will occur rapidly in the presence of an iron-chrome catalyst at temperatures of 400 ^{o}C or greater to produce water and carbon monoxide (as a side product) from carbon dioxide and hydrogen, produced from steam reforming and partial oxidation. Additionally, this process can be recovered at high temperature. The reaction is summarised by

$$CO_2 + H_2 \quad \Leftrightarrow \quad CO + H_2O \qquad \Delta H_{298K} = \ -42.2 \ kJ/mol \qquad (2.7)$$

However, That is, the CO produced by this reaction is discarded while the water is electrolyzed to produce oxygen (the net product), and hydrogen which can be recycled to reduce more CO_2. This reaction has an equilibrium constant of 0.1 even at temperatures of 400 ^{o}C or above, so it must be fed with either a hydrogen-rich or a carbon dioxide-rich mixture to ensure satisfactory results. Excess hydrogen (or excess carbon dioxide) is captured from the exhaust with a filtering membrane and fed back into the reactor.

2.5 Methanation

Methanation combines carbon monoxide from the reverse water gas shift reaction and hydrogen to produce methane, CH_4, the major by-product in reforming system. To minimize the methane content in the synthesis gas while simultaneously maximizing the hydrogen-yield, the reformer should be operated with a higher steam/carbon ratio than theoretically necessary.

$$CO + 3H_2 \quad \Leftrightarrow \quad CH_4 + H_2O \qquad \Delta H_{298K} = \ -206.11 \ kJ/mol \quad (2.8)$$

CHAPTER III

LITERATURE REVIEWS

Hydrogen is widely considered as an alternative fuel because it has the highest energy content per unit of weight, compared with any other known fuels. Hydrogen can be efficiently produced from a variety of resources such as biomass, natural gas and other hydrocarbons in industrial reformers. A number of investigations focusing on simulation and experimental studies for hydrogen production will be discussed in this chapter.

3.1 Hydrogen production processes

A thermodynamic study of a reforming process for hydrogen production has been widely reported in literatures. Most of these works concentrated on the investigation of the characteristics of reforming reactions in the system, which use different type of fuel and processes.

3.1.1 Partial oxidation process

Costa et al. (2008) studied the effect of support nature on the performance of Pd catalysts during partial oxidation of ethanol. From the results, hydrogen, carbon monoxide and acetaldehyde formation was favored on Pd/CeO_2, whereas CO production was facilitated over Pd/Y_2O_3 catalyst. According to the reaction mechanism, some reaction pathways are favored depending on the support nature, which can explain the differences observed on products distribution. The production of acetate species was promoted on Pd/Y_2O_3, but the acetaldehyde preferentially desorbed and/or decomposed on Pd/CeO_2. Moreover, at the reaction temperature lower than 773 K, Pd/CeO_2 exhibited the highest selectivity to hydrogen, carbon dioxide and acetaldehyde, whereas the CO formation was favored on Pd/Y_2O_3 catalyst. On the other hand, at elevated temperatures, Pd/CeO_2 exhibited the highest selectivity to hydrogen and lower formation of methane than Pd/Y_2O_3.

Shuhong et al. (2008) investigated the catalytic partial oxidation of methane (CPOM) to produce synthesis gas (syngas) in a fixed-bed distributor. The axial temperature and gas composition profiles along the Ni or Rh-based catalyst bed were measured at different conditions. As the oxygen was distributed radially into the catalyst

bed through several rows of holes arranged at the special zone of an oxygen distributor, a micro environment maintaining low oxygen to methane molar ratio (0.10–0.22) was provided. As a result, the hot spot phenomena appeared at the entrance of the catalyst bed were effectively controlled. This caused a more uniform temperature profile along the catalyst bed, which is beneficial to the stability of catalyst and the safety of reactor operation. The results showed that the thermodynamic equilibrium of CPOM reaction system was not changed whether or not changing the ways of air feeding by using the oxygen-distributor. Combining the measurements of temperature profile and species profile, the reaction path of the CPOM reaction might have some changes at lower oxygen to methane molar ratio when using the oxygen distributor.

Wenju and Yaquan (2008) reported thermodynamic equilibrium of ethanol partial oxidation by using Gibbs free energy minimization method for hydrogen production in the range of molar feed ratio (Oxygen/Ethanol (O/E) = 0-3, Nitrogen/Ethanol (N/E) = 0-100), the reaction temperature (500-1400 K), and system pressure (1-20 atm). The optimal operation conditions were obtained at 1070-1200 K, O/E molar ratio of 0.6-0.8, and atmospheric pressure. Under the optimal conditions that the complete conversion of ethanol and no coke formation were observed, the hydrogen yield of 86.28-94.98% can be achieved whereas the mole fraction of carbon monoxide of 34.69-38.64 % was found. Increasing operating pressures has a negative effect on the hydrogen yield. The formation of coke is favored at lower temperatures and lower O/E molar ratios.

3.1.2 Steam reforming process

Lwin et al. (2000) studied thermodynamic equilibrium of methanol steam reforming as a function of temperatures (360-573K), steam to methanol molar feed ratios (0-1.5), and atmospheric pressure. The equilibrium concentrations were calculated by the method of direct minimization of Gibbs free energy. Carbon and methane formations were not considered when this process occurs at 1 atm, 400 K and a molar feed ratio of 1.5 with a hydrogen-yield 2.97 mole per mole of methanol. At the feed ratios greater than 1.5, carbon monoxide and di-methyl-ether concentrations can be further reduced. However, hydrogen yield is not raised above its theoretical limit of 3 moles per one mole of methanol.

3.1.3 Autothermal reforming process

Zahedi et al. (2009) explored an autothermal reforming to produce synthesis gas. Two sections, a combustion section (non-catalytic partial oxidation) and a catalytic bed section (catalytic steam reforming) were investigated. In the combustion section,

temperature and compositions were predicted using 108 simultaneous elementary reactions considering 28 species whereas in the catalytic bed section, a one-dimensional heterogeneous reactor model was used for simulations. From the results, it was found that operation at higher temperatures increases the rate of reactions and reduces the operating time required to approach the equilibrium condition. Since more fraction of methane is converted to undesired products such as H_2O and CO_2, the conversions closed to equilibrium lead to the reduction of relative H_2 and CO production. Feed Methane to oxygen ratio has a direct effect on the reaction temperature. To have higher temperatures and reaction rate, the concentration of oxygen in feed should be increased. However, an increase in the oxygen concentration reduces the H_2/CO molar ratio of a product stream.

Li et al. (2008) studied thermodynamic equilibrium of methane autothermal reforming by Gibbs free minimization for methane conversions, H_2 yield and coke deposition as a function of water to methane molar ratio, carbon dioxide to methane molar ratio, oxygen to methane molar ratio, reforming temperature and pressure system. The results showed that coke elimination should be done by increasing the reaction temperatures in CO_2 reforming and increasing the steam fed in steam reforming. Moreover, the O_2/CH_4 ratios should be higher than 0.4 or H_2O/CH_4 ratios higher than 1.2 for oxidative steam reforming when the reaction temperature is higher than 700˚C. The optimal $CH_4/CO_2/O_2$ feed ratios 1:0.8-1.0:0.1-0.2 were corresponding to the reaction temperature higher than 800˚C.

Vagia et al. (2008) investigated a thermodynamic analysis of an autothermal steam reforming of bio-oil components: acetic acid, acetone, and ethylene glycol, in the range of temperature (400-1300K), steam to fuel ratio (1-9) and pressure (1-20 atm) values. The equilibrium concentrations were calculated by Gibbs free energy minimization. The maximum hydrogen yield is achieved at 900K. The optimal steam to fuel ratio value for the acetic acid and the ethylene glycol is 6 and for acetone is 9. The optimal ratio of oxygen to fuel is 0.33, 0.26, and 0.62 for acetic acid, ethylene glycol, and acetone, respectively.

Semelsberger et al. (2004) presented the thermodynamic analyses of autothermal processes using five fuel; natural gas, methanol, ethanol, dimethyl ether, and gasoline as raw materials. The analyses were carried out to determine the equilibrium product concentrations at the temperature range of 300-1000 K, pressures range of 1-5 atm, and the water to fuel molar ratios varied between 1-9 times of the stoichiometric value. The result showed that the optimum conditions for natural gas reforming were found on the

water to fuel molar ratio of 4 at 1000 K. For cases of methanol, ethanol, dimetyl ether, and gasoline feeds, the optimal ratio of water and fuel are 1.5, 4, 4, and 9 at 400K, 540K, 420, and 800 K, respectively. Moreover, the calculation also presented that the oxygen containing substances (methanol, ethanol and dimethyl ether) required lower operating temperatures than the non-oxygenated fuels (natural gas and gasoline).

3.1.4 Comparison between different processes

Gerd and Viktor (2008) studied thermodynamics of hydrogen production from ethanol by steam-reforming, partial-oxidation and auto-thermal reforming as a function of steam to ethanol molar ratio (0.00–10.00), oxygen to ethanol molar ratio (0.00–2.50) and temperatures (200–1000 ^{o}C) at atmospheric pressure. The equilibrium concentration was calculated by Gibbs enthalpy minimization. The results showed that ethanol can be fully converted at low temperatures and the major product was methane, which changed to hydrogen with increased temperatures. At elevated temperature, carbon monoxide content increased which was in accordance with the water gas shift reaction. Coke formation was a serious issue, especially at low steam to ethanol (S/E) ratios. Steam reforming gave the highest hydrogen yield, which nearly achieved the theoretical value at a high steam to ethanol ratio. Pure partial oxidation showed the similar trends of hydrogen and carbon monoxide content with temperature and oxygen to ethanol (O/E) ratio. Moreover, a low hydrogen yield and the avoidance of coke formation demand on high temperatures or high O/E ratios. Increasing O/E-ratio from 0.00 to 0.75 in autothermal reforming showed no strong effect on the hydrogen and carbon monoxide formation at temperatures below 600 ∘C and over the whole S/E-ratio range. Autothermal operation reduced the coke-formation and reduced energy demand for the reforming process.

Seo et al. (2002) studied the characteristics of three different types of a methane reforming process including steam methane reforming, partial oxidation and autothermal reforming as a function of the molar feed ratio, the operating pressure and temperature and the preheat temperature of reactant by using AspenPlus^{TM}. The thermodynamic equilibrium was calculated by the method of minimizing the Gibbs free energy. From the results, the optimum steam to carbon ratio of steam reforming process was 1.9, the optimum air to carbon ratio of the partial oxidation process was 0.3 at a preheating temperature of 312 ^{o}C. For autothermal reforming process, the optimum air to carbon ratio and steam to carbon ratio was 0.29 and 0.35, respectively at the preheating temperature of 400 ^{o}C. However, the maximum and minimum methane consumption was found in steam reforming process and partial oxidation, respectively.

3.2 Use of glycerol for hydrogen production

There are various processes applied to produce hydrogen from glycerol, but three major technologies: steam reforming (SR), partial oxidation (POX), and autothermal reforming (ATR), are widely studied.

Nianjun et al. (2008) investigated the production of hydrogen from a glycerol via aqueous phase reforming over Pt catalysts by considering the effect of metal loading and operation conditions. The reaction pathways showed that hydrogen generation is accompanied by side reactions to form alkane and liquid products. Series of Al_2O_3 supported Pt catalysts were prepared and tested for glycerin aqueous reforming under various conditions. The catalyst with 0.9 wt% Pt has the best performance for hydrogen generation. Higher reaction temperatures facilitated reforming process to produce higher hydrogen yield. The reaction pathways disclosed selective reactions for hydrogen production over platinum catalyst were accompanied with other parallel reactions (such as dehydration and hydrogenation) and further methanation.

Nianjun et al. (2007) studied the thermodynamic property of a glycerol aqueous reforming process to generate hydrogen for fuel cells with three ways of processing. Autothermal reforming, aqueous hydrogen peroxide reforming, and the water aqueous reforming process were investigated and compared. The results showed that the high fraction of hydrogen can be occurred when the side reaction, methanation, is limited kinetically. Comparison of these three kinds of processes indicated that the water aqueous reforming gave the highest hydrogen-yield, followed by the autothermal reforming and aqueous hydrogen peroxide reforming process.

Nianjun et al. (2007) also studied a thermodynamic of polylols reforming to generate hydrogen-rich gas. Polylols can be converted into carbon dioxide and hydrogen via aqueous-phase reforming with co-existence of low level of carbon monoxide due to a reverse water gas shift (R-WGS) reaction and subsequently, CO and/or CO_2 and H_2 react to form CH_4 via the side reaction of methanation which decreased hydrogen production in products. Matlab was employed to calculate the reaction heat, equilibrium constant and equilibrium molar fraction of each component through solving the non-linear equations. The calculation results suggested that the polylols reforming is endothermic but should be carried at low temperature to give very low level of CO content in the product gas. The results also demonstrated that low temperature favored the methanation, which should be limited kinetically during the operation. In addition, the system pressure, slightly higher

than the saturation water pressure, was unfavorable to the R-WGS reaction but favorable to the low level of CO content.

Sushil et al. (2007) analyzed thermodynamic equilibrium of glycerol steam reforming by using the direct minimization of the Gibbs free energy. Simulations were performed using Mathcad version 11. Steam reforming of glycerol for hydrogen production involves complex reactions. As a result, several intermediate by-products were formed and end up in the product stream affecting the final purity of the hydrogen produced. Furthermore, the yield of the hydrogen depends on several process variables, such as system pressure (1–5 atm), temperature (600–1000 K), and ratio of reactants (water to glycerol molar feed ratio 1:1–9:1). The study revealed that the best conditions for producing hydrogen was at a temperature higher than 900 K, atmospheric pressure, and a molar ratio of water to glycerol of 9:1. Under these conditions, methane production was minimized, and the carbon formation was thermodynamically inhibited. The upper limit of moles of hydrogen produced per mole of glycerol is 6 whereas the stoichiometric limit of moles of hydrogen is 7. Although water-rich feed increased the hydrogen production, a significant amount of unreacted water was the product stream. The behavior of this system was very similar to that of steam reforming of ethanol.

Sushil et al. (2007) compared a thermodynamic equilibrium analysis with experimentation for the hydrogen production from the steam reforming process of glycerin as a function of pressure (1-5 atm), temperature (600-1000 K), and water to glycerin feed ratio (1:1-9:1). The equilibrium concentrations of different compounds were calculated by the method of direct minimization of the Gibbs free energy. The study revealed that the best conditions for producing hydrogen were found at the temperature over 900 K, atmospheric pressure, and a molar ratio of water to glycerin was 9:1. Under aforementioned conditions, methane production was minimized and the carbon formation is thermodynamically inhibited. Experimental results over the Ni/MgO catalyst were compared against the results obtained from thermodynamic analysis and the results were still far from thermodynamic equilibrium.

Zhang et al. (2007) revealed the hydrogen production from ethanol and glycerol steam reforming over ceria-supported Ir, Co and Ni catalysts with respect to the nature of the active metals and the reaction pathways. For ethanol steam reforming, ethanol dehydrogenation to acetaldehyde and ethanol decomposition to methane and carbon monoxide were the primary reactions at low temperatures, depending on the active metals. At higher temperatures, all the ethanol and the intermediate compounds, like

acetaldehyde and acetone, were completely converted into hydrogen, carbon oxides and methane. Steam reforming of methane and water gas shift became the major side reactions. The Ir/CeO_2 catalyst was significantly more active and selective toward hydrogen production, and the superior catalytic performance was interpreted in terms of the intimated contact between Ir particles and ceria based on the ceria-mediated redox process. Additionally, hydrogen production from steam reforming of glycerol was also examined over these ceria-supported metal catalysts, and the Ir/CeO_2 catalyst again showed quite promising catalytic performance with hydrogen selectivity of more than 85 % and 100 % glycerol conversion at 400 ^{o}C.

3.3 The optimal condition for hydrogen production

The experimental investigation of bio-ethanol autothermal reforming and water-gas shift processes for hydrogen production and regression analysis of the data was performed in Markovaa et al. studied (2009). The experimental conditions were selected based on the previous experience in research of ATR processes at Fraunhofer Institute for Solar Energy systems and results of chemical equilibrium simulations done with software ChemCAD. The main goal was to obtain regression relations between the most critical dependent variables in the gas reformer and independent factors such as molar feed ratio, inlet temperature of reactants into reforming process, pressure and temperature in the ATR reactor. Purpose of the regression models was to provide optimum values of the process factors that gave the maximum amount of hydrogen. The optimization results showed that within the considered range of the process factors the maximum hydrogen concentration of 42 dry vol. % and yield of 3.8 mol/mol ethanol of the ATR reactor could be achieved at S/C of 2.5, O/C of 0.20–0.23, pressure of 0.4 bar, T_{ATRin} at 230 $\circ$C and T_{ATR} at 640$\circ$C.

Song et al. (2008) studied about the energy demand from the autothermal reaction obtained by coupling the endothermic steam reforming process with the exothermic partial oxidation of methane. From the thermodynamic calculation, the autothermal reaction could be optimized for maximizing the hydrogen production by decreasing the O/M (oxygen to methane) ratio and increasing the S/M (steam to methane) ratio. Moreover, this work showed that the heat of the autothermal reaction was sufficient to bring the membrane to the temperature required for hydrogen permeation. It was found that the optimum condition for the purpose of maximizing the hydrogen production by decreasing the O/M ratio and increasing the S/M ratio was shown in this process.

Alessandra (2007) revealed the energetic optimization of a proton exchange membrane fuel cell integrated with a steam reforming system using ethanol as fuel. In order to obtain high hydrogen production, a thermodynamic analysis of the steam reforming process had been carried out and the optimal operating conditions had been defined. Moreover, the overall efficiency of the PEMFC-SR system also investigated as a function of the fuel utilization factor and the effects of the anodic off-gas recirculation. The results showed that the amount of hydrogen produced determined the efficiency of the fuel processor because it was defined as the ratio of the higher heating value of the total quantity of hydrogen in the reformate to the higher heating value of the ethanol used in the fuel processor, when no additional external heat was considered in the energy balance.

Zhixiang et al. (2006) presented the hydrogen production using hydrocarbons as raw material from autothermal reforming process. Liquefied petroleum gas, with propane as the main component, was a promising fuel for on-board hydrogen producing systems in fuel cell vehicles and for domestic fuel cell power generation devices. In this article, propane ATR process was studied and operation conditions were optimized with PRO/II from SIMSCI for proton exchange membrane fuel cell application. In the ATR system, heat in the hot streams and cold streams was controlled to be in balance. Different operation conditions were studied and drawn in contour plots. One operation point was chosen with the following process parameters: feed temperature for the ATR reactor was 425 ^{o}C, steam to carbon ratio S/C was 2.08 and air-flow was 0.256. The thermal fficiency for the integrated system was calculated to be as high as 84.0 % with 38.27 % H_2. The operation conditions of a propane ATR system were optimized with heat balance in the system by means of the simulation software package PROAI. The simulation results were drawn in contour plots by varying the steam to carbon ratio and ATR feed temperature. In such a way operation regions unsuitable for the system operation could be figured out, liked too high temperature regions for the system and carbon forming region, the optimum operation region with the highest efficiency could be identified.

The objective of Chaniotis et al. (2005) was the investigation and optimization of a micro-reformer for a fuel cell unit based on catalytic partial oxidation using a systematic numerical study of chemical composition and inflow conditions. The optimization targeted hydrogen production from methane. Additionally, the operating temperature, the amount of carbon formation and the methane conversion efficiency were taking into account. The fundamental investigation was first based on simplified reactor

models (surface perfectly stirred reactor (SPRS)). As a consequence, the residence time of the process was taken into account, which meant that the products were not necessary in equilibrium. A region where all the targeted operating conditions were satisfied and the yield of hydrogen is around 80% is identified. The analysis focused on the inlet conditions such as temperature, velocity and chemical composition for a typical monolith configuration. In the simulations detailed surface chemistry mechanism was adopted in order to capture all the important features of the reforming process. The finite radial diffusion of the Navier–Stokes model compared to the infinite diffusion of the SPSR seem not be important in our case study, since the residence time in the channel was a multiple of the radial diffusion time. The hydrogen production is strongly depended on the equivalence ratio between 0.6 and 1.0 was shown to produce high values of hydrogen yield which approximated 70–80% with realistic operating conditions, inlet velocity at 1ms−1 and inlet temperature at 875 K.

The optimization of the combined carbon dioxide reforming and partial methane oxidation over a 1% $Pt-Al_2O_3$ catalyst to produce synthesis gas with hydrogen/carbon monoxide ratio close to 1 was studied by Ariane et al. (2001). The study was performed with the help of experimental design and two mathematical modeling approaches, empirical and phenomenological. The empirical modeling approach was found to be more efficient, simpler and led to better results than those obtained with the phenomenological model approach. Therefore, the empirical modeling was used for optimization of the process operation conditions. At an oxygen/methane ratio of 0.55 and temperature of 950 ^{o}C, optimized process conditions were obtained with complete methane conversion, maximum carbon monoxide selectivity of 43% and minimum hydrogen/carbon monoxide ratio of 1.3, in absence of water.

CHAPTER IV

METHODOLOGY

Three different reforming processes, glycerol steam reforming, partial oxidation and autothermal reforming are described in this part. In this process combines with three reactors, an evaporator, a reformer and a water gas shift reactor. The temperature and pressure of streams inlet are fixed at 273 K and 1 atm respectively. And then, the inlet streams are heated to 580 K for convert water and glycerol from aqueous phase into gas phase by evaporator. The different reformers generate synthesis gas, hydrogen and carbon monoxide, at the temperature range between 600 and 1200 K. For using in high temperature PEM fuel cell, the products are cooled-down to 450 K. Because of limitation of the different energy transfer in heat exchanger, gases product are cooled-down into 480 K before. In heat exchanger, the energy cooled-down any products is used to heat inlet glycerol for reducing energy demand at the evaporator. Because fuel cell electrodes can tolerate only very low concentrations of carbon monoxide, the water gas shift reactor is added to convert synthesis gas to hydrogen and carbon dioxide at the same condition.

4.1 Description of glycerol steam reforming process

The endothermic process for hydrogen production, using glycerol as raw material is demonstrated. The system shown in Figs. 4.1 and 4.2 is based on a steam reforming reactor, which is investigated by performing a thermodynamic equilibrium analysis for the products and reactants. The reformer has three reactions which are steam reforming reaction, reverse water gas shift reaction and methanation reaction.
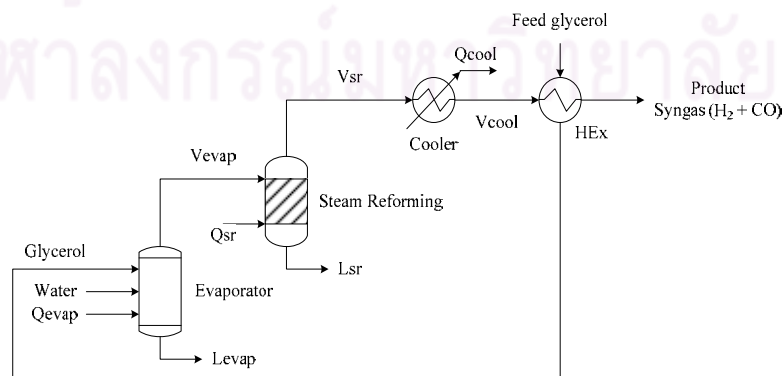
Fig. 4.1 A flow diagram of the steam reforming system components for synthesis gas production.
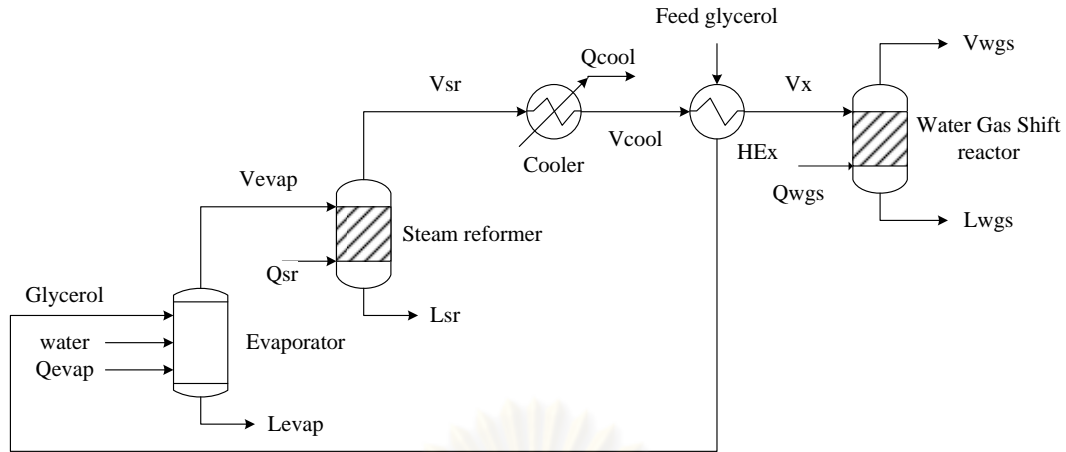
Fig. 4.2 A flow diagram of the steam reforming system components for hydrogen and carbon dioxide production.

The process involves two main-reactors for synthesis gas production, an evaporator (Evap) and a steam reformer (SR). The water gas shift reactor (WGS) is added in the process for convert CO into H_2 and CO_2 production. The simulation is solved by using HYSYS simulation software.

Inlet streams

Glycerol and water as a liquid phase are fed into the system at 273 K and 1 atm, and then the streams are heated to vapor phase by evaporator. The proportion of steam-to-glycerol (S/G) molar feed ratio can be written as:

$$\text{Water-to-glycerol ratio (S/G)} = \frac{\text{Molar flow rate of glycerol}}{\text{Molar flow rate of steam}} \quad (4.1)$$

In this study, the SR process operates between 600 and 1200 K at atmospheric pressure. The ratio of streams feed inlet is varied from 1 to 9. At higher feed ratio, the total energy demand is shapely increase but the different maximum hydrogen concentration is slightly increased.

4.2 Description of glycerol partial oxidation process

Partial oxidation is an exothermic reaction, releasing energy as it proceeds. Because of higher hydrogen production from the process, WGS is added in this study. Fig. 4.3 shows a flow diagram of the glycerol partial oxidation system. The process involves three reactors, an evaporator, a partial oxidation reformer and a water gas shift reactor. Since the efficiency of the reformer is considered, the system is as same as the steam reforming process. The reformer has three reactions which are partial oxidation reaction, reverse water gas shift reaction and methanation reaction.
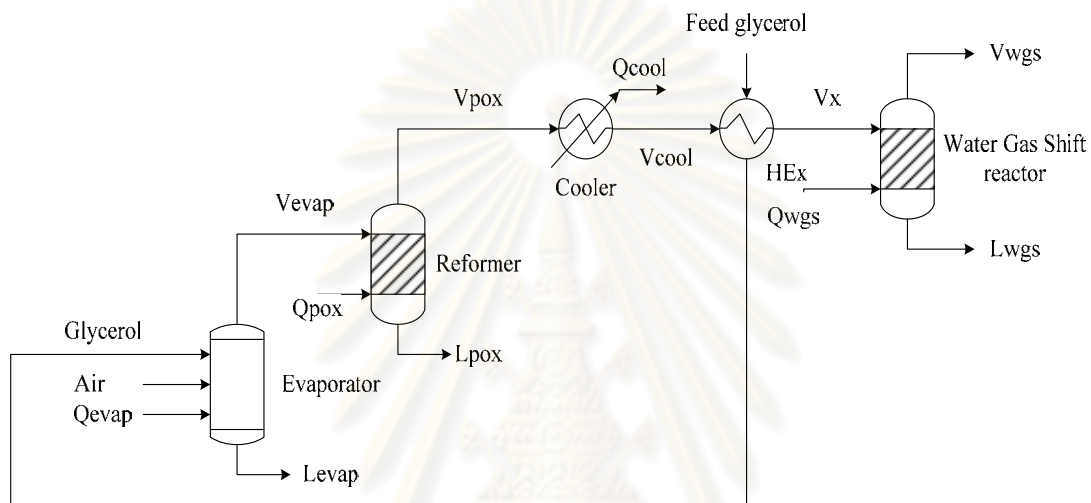
Fig. 4.3 A flow diagram of the partial oxidation system components for hydrogen and carbon dioxide production.

Inlet streams

Since pure oxygen is not economical, air as an oxygen carrier is used in this part. Glycerol as a liquid phase fed into the system at 273 K and heated by evaporator to 580 K is combined with air that including 21 mol% of oxygen and 79 mol% of nitrogen at vapor phase. The proportion of oxygen-to-glycerol (O/G) molar feed ratio can be written as:

$$\text{Oxygen-to-glycerol ratio (O/G)} = \frac{(\text{Molar flow rate of oxygen}) / 0.21}{\text{Molar flow rate of glycerol}} \quad (4.2)$$

The gas outlet streams from the POX reactor are varied temperature in the range of 600-1200 K, which corresponds to O/G molar ratio of 0.5-3. At higher feed ratios make the POX reaction occurs lower than reverse water gas shift reaction. And at lower feed ratio, a lot of the total energy demand is released but the different maximum hydrogen concentration is slightly increased.

4.3 Description of glycerol autothermal reforming process

        The autothermal reforming process combines the steam reforming and partial oxidation together. Steam reforming is an endothermic reaction, absorbing energy as it proceeds. Vaporizing water to form steam is a further energy requirement of this process, usually supplied by partial combustion of the fuel. A flow diagram of the glycerol autothermal reforming system is shown in Fig. 4.4. The ATR process involves three reactors as same as SR and POX system.
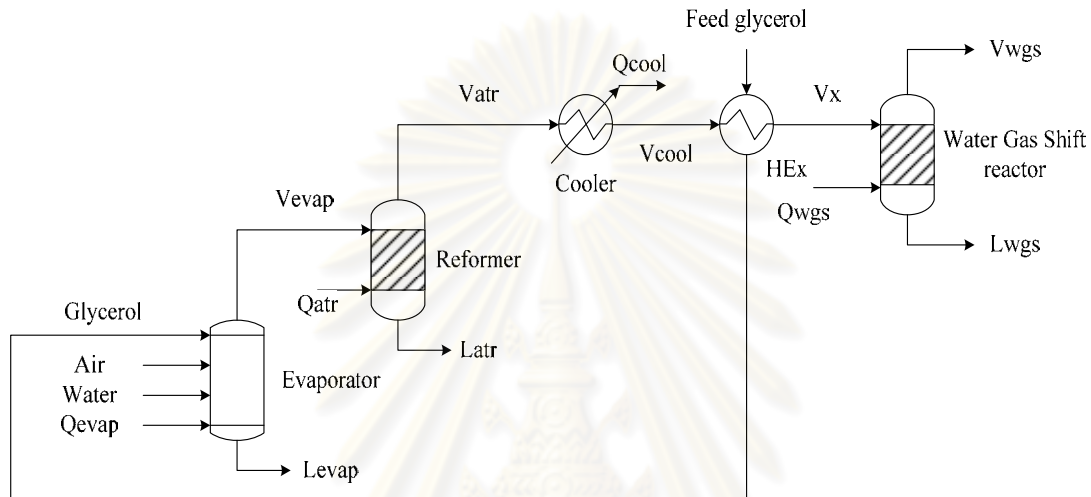
Fig. 4.4 A flow diagram of the autothermal reforming system components for hydrogen and carbon dioxide production.

Inlet streams

        Glycerol, water and air are separately fed into the system at 273 K. Glycerol and water are heated by evaporator and then combined with air at vapor phase. The proportion of steam-to-glycerol molar ratio is written in Eq. 4.1 and the proportion of oxygen-to-glycerol molar ratio is written in Eq. 4.2. The reformer has four reactions which are steam reforming reaction, partial oxidation reaction, reverse water gas shift reaction and methanation reaction.

        The streams production from the ATR reactor are generated at the temperature range of 600-1200 K which corresponds to S/G in range of 1-9 and O/G in range of 0.5-2.

5.4 Optimization for hydrogen production

For each of R ratio, there is an optimal temperature for reformer operation to provide the maximum H_2 yield in the range of temperature 600-1200 K. The result is solved by HYSYS-Optimization software. On this program, the optimizer is used to find the operating conditions which maximize hydrogen generated. The optimizer contains a spreadsheet for defining the objective function as well as any constraints. To consider the efficiency of the different reformer, an objective function in this work is maximized hydrogen production from the reformer.

CHAPTER V

RESULTS AND DISCUSSION

This chapter presents the entirely feasible results of the different glycerol reforming, steam reforming, partial oxidation and autothermal reforming, as a thermodynamic point of view. The system of glycerol reformer involves a set of response reactions which have different relative fractions at the different operative conditions. Because the maximum hydrogen production may be affected from each response reaction, the generated hydrogen depends on the operative condition i.e., reaction temperature and stream molar feed ratio.

5.1 Steam reforming for hydrogen and synthesis gas production

The effect of key parameters for glycerol steam reforming reaction i.e., steam-to-glycerol (S/G) molar feed ratio (R_{sr}) and operating temperature on the equilibrium compositions is discussed in this part. At the standard condition, the R_{sr} ratio of 3 based on stoichiometric and reaction temperature at 600 K based on the minimum temperature that can be occurred are studied. The result at standard condition before parameters variation is shown in tables 5.1 and 5.2. On table 5.2, the WGS reactor is added in the system to convert CO into CO_2 and H_2.

Table 5.1 The result of SR process at the standard condition

Molar flow of inlet stream (kmol/h)	
glycerol	1
water	3
Inlet stream feed temperature (K)	273
System pressure (atm)	1
Steam reformer	
inlet temperature (K)	580
outlet temperature (K)	600

Table 5.1 The result of SR process at the standard condition (cont.)

Steam reformer	
products composition (kmol/h)	
H_2	0.3480
CO_2	1.3336
CO	0.0046
CH_4	1.6618

Table 5.2 The result of SR process with WGS is added at the standard condition

Water gas shift reactor	
inlet temperature (K)	450
outlet temperature (K)	450
products composition (kmol/h)	
H_2	0.3523
CO_2	1.3379
CO	0.0003
CH_4	1.6618

5.1.1 Effect of reaction temperature

In this work, the reforming temperature is studied between 600 and 1200 K. At a fixed of S/G molar feed ratio, the amount of hydrogen and carbon monoxide generated from SR reaction increase with the increasing temperature until it reaches the highest H_2 production and then the H_2 yield decreases because the reverse water gas shift occurs better than steam reforming at high temperature. The CO_2 concentration also increases at low temperature but decreases at a higher temperature for convert CO_2 into CO in the shift reaction. So that, the only CO content increases with increasing temperature. However the methanation which is a side reaction from SR process can be occurred at lower temperature and then decreases with increasing temperature because it is an exothermic reaction. Fig. 5.1 shows the variation of the SR products with the constant S/G molar ratio of 3 at the operating temperature range between 600 and 1200 K and atmospheric pressure.
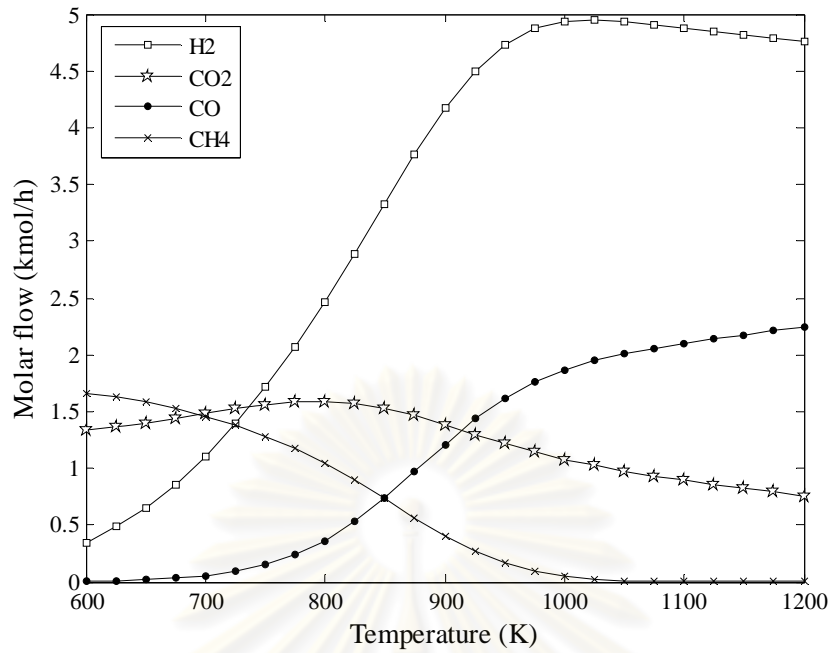
Fig. 5.1 Plot of thermodynamic equilibrium molar flow of each component based on S/G molar feed ratio of 3

5.1.2 Effect of the steam-to-glycerol (S/G) molar feed ratio, R_{sr}

The effect of R_{sr} ratio varied from 1 to 9 for each operating temperature in SR reactor at the equilibrium condition is investigated. The hydrogen yield over changing S/G ratio is shown in Figs. 5.2 and 5.3. All of production will be also increased with the increasing stream inlet (Eq. 2.2), so that a higher R_{sr} ratio is favorable for higher glycerol conversion and H_2 formation. Moreover, at a lower ratio, the maximum of H_2 produced is derived from steam reforming at high reaction temperature and then decreases with higher feed ratio. Meaning that, the highest quantity of H_2 is generated at the excess water condition. The maximum of H_2 production is found to be 6 kmol/h and R_{sr} ratio of 9 at 950 K. But the molar fraction (Fig. 5.3), can be written as Eq. 5.1, is found to be lower because of the unreacted of excess water. Since the water inlet is inadequate, the only R_{sr} ratio of 1 produces higher fraction content of hydrogen at all of the temperature range.

$$\text{Mole fraction of } H_2 = \frac{\text{Moles of } H_2 \text{ in the products}}{\text{Moles of all products}} \qquad (5.1)$$
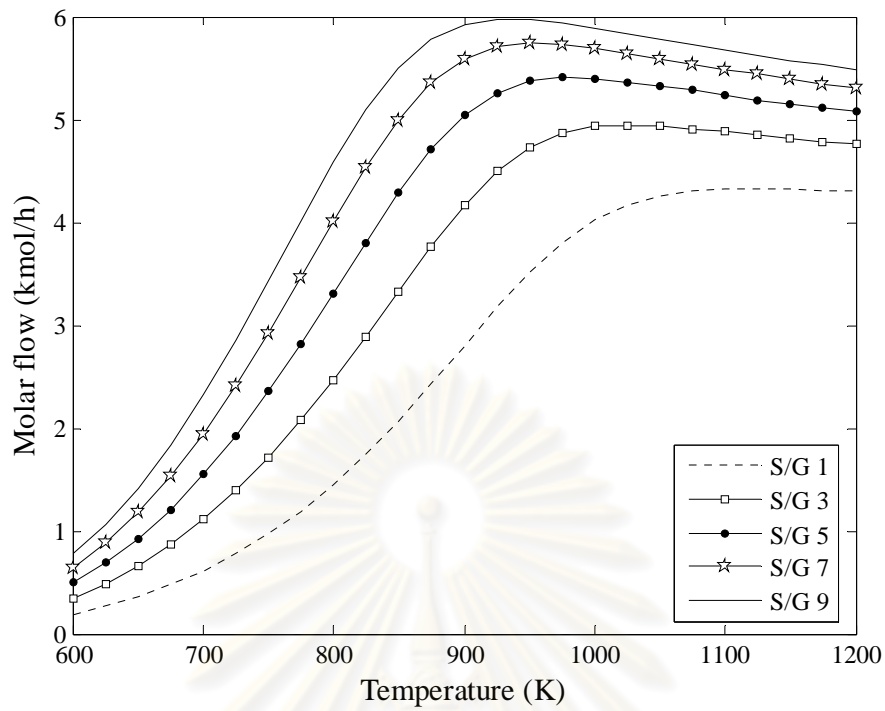
Fig. 5.2 Plot of thermodynamic equilibrium molar flow of hydrogen content at various ratios as a function of temperature at atmospheric pressure when steam reforming is employed
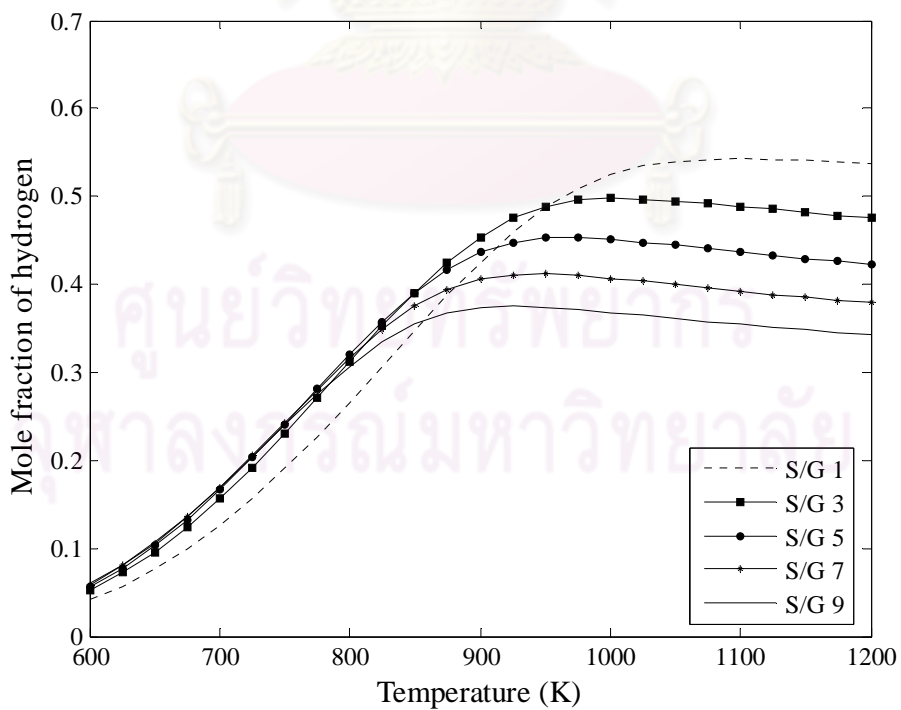
Fig. 5.3 Plot of thermodynamic equilibrium molar fraction of hydrogen at various ratios as a function of temperature at atmospheric pressure when steam reforming is employed

Fig. 5.4 shows the effect of R_{sr} ratio on the equilibrium compositions in SR reactor at 1 atm. To analyze the thermodynamic equilibrium of stream outlet, CO, CO_2 and CH_4 are found as by-products. Because a higher R_{sr} ratio makes the SR reaction occurs better than R-WGS and methanation reaction, the CO_2 concentration is the same tendency as H_2 formation. But the CO and CH_4 concentrations are reverse. Finally, CH_4 concentration drops to zero at 1100 K.
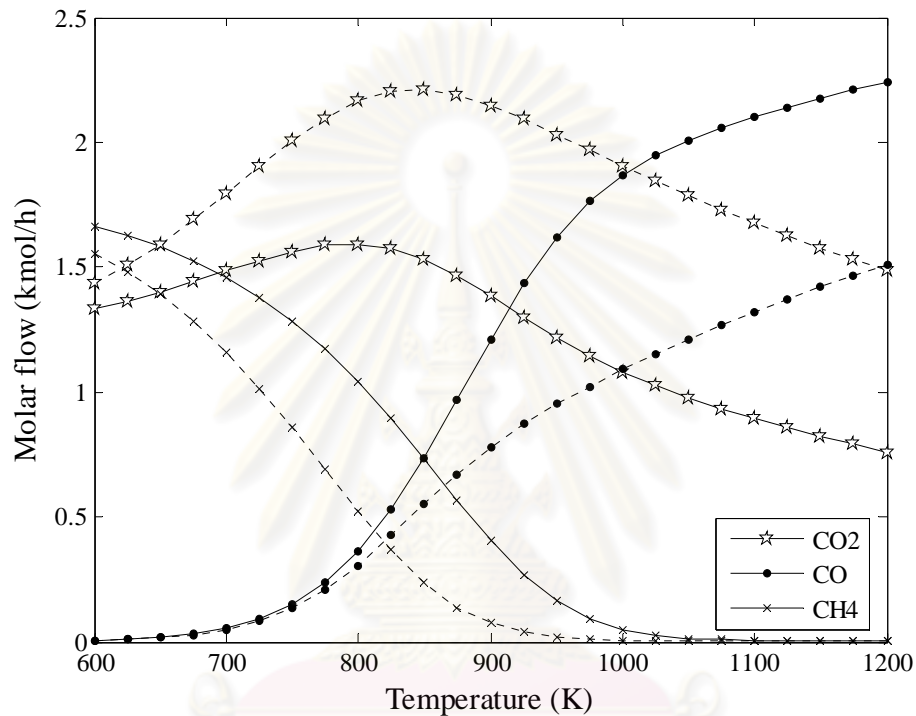
Fig. 5.4 Plot of thermodynamic equilibrium molar flow at R_{sr} ratio of 3 (solid line) and 9 (dashed line) as a function of temperature at atmospheric pressure when steam reforming is employed

5.1.3 Effect of water gas shift reactor

Because of the limitation of carbon monoxide content using in fuel cell, water gas shift reactor is added in this section for convert CO into CO_2 and H_2. From the result shown in Figs. 5.5-5.7, most of the compositions have a tendency to the only steam reforming reactor at the temperature lower than 1000 K. For all case of this study, the H_2 and CO_2 production are remaining constant at the final because the shift reactor completely converts CO from the reformer into CO_2 and H_2. Meaning that, the CO concentration drops to zero in all cases. By-product, methane, is not affected in this case since the WGS reactor has only WGS reaction.
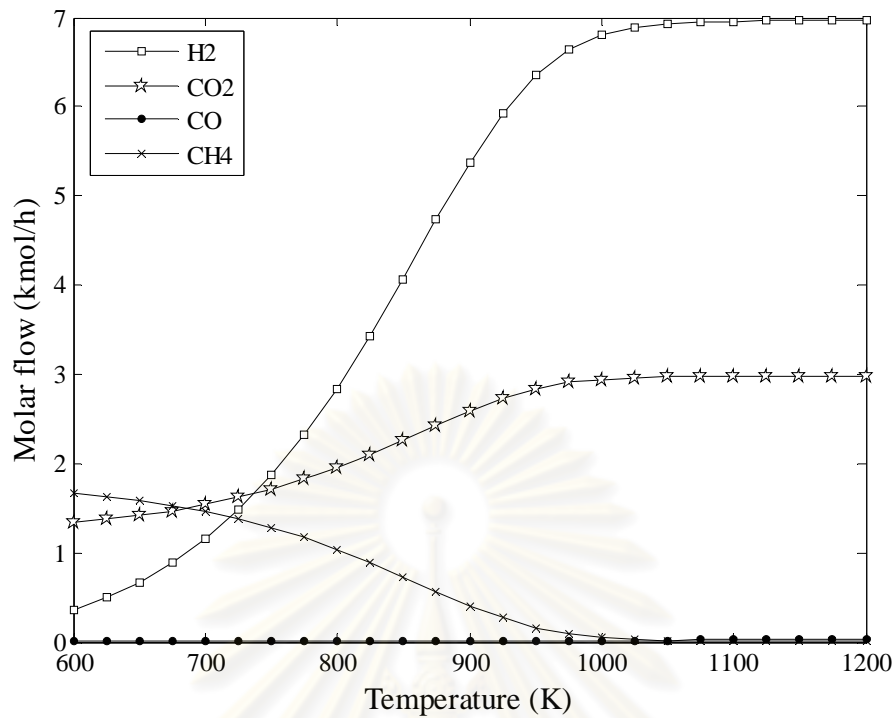
Fig. 5.5 Plot of thermodynamic equilibrium molar flow based on R_{sr} ratio of 9 at 1 atm with WGS reactor is added
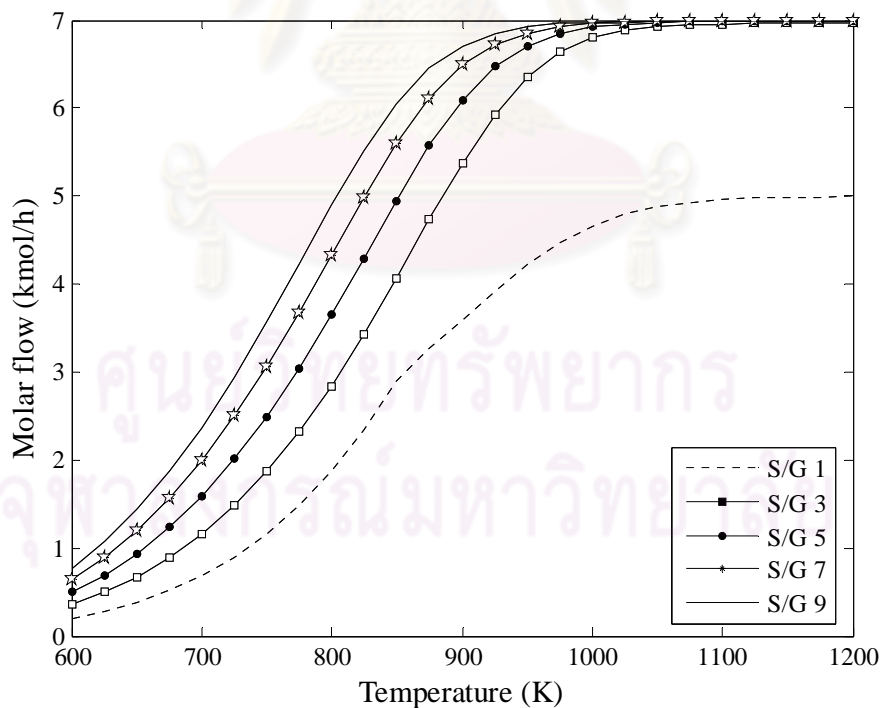
Fig. 5.6 Plot of thermodynamic equilibrium molar flow of hydrogen at various ratios as a function of temperature at atmospheric pressure when WGS reactor is added
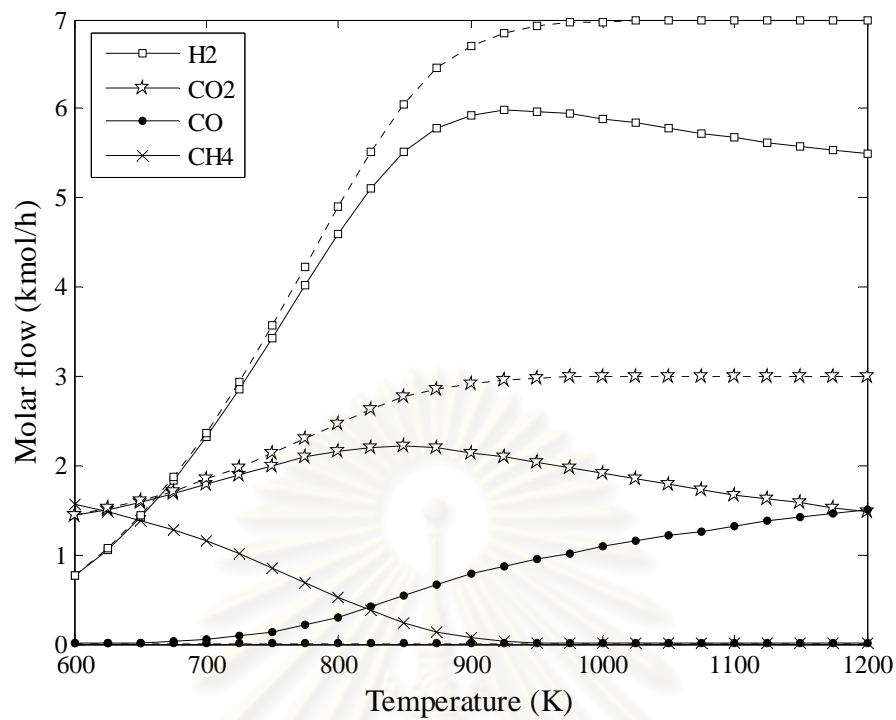
Fig. 5.7 Plot of thermodynamic equilibrium molar flow from only steam reforming reactor (solid line) and added WGS reactor (dashed line) as a function of temperature based on R_{sr} ratio of 3

5.2 Partial oxidation for hydrogen production

　　　　Since pure oxygen is not economical, air as an oxygen carrier is used in the partial oxidation process. A major disadvantage of any partial oxidation or air addition is the nitrogen dilution of the hydrogen containing effluent. This nitrogen dilution is deteriorating full cell operation, because increased nitrogen content makes the open-circuit voltage of the fuel cell lower. The effect of key parameters of partial oxidation reaction i.e., oxygen-to-glycerol (O/G) molar feed ratio (R_{pox}) and reaction temperature on the equilibrium compositions is studied and discussed in this part.　　　　At　　　　the standard condition, the R_{pox} ratio of 1.5 based on stoichiometric and reaction temperature at 600 K based on the minimum temperature that can be occurred are studied. The result at standard condition before parameters variation is shown in tables 5.3 and 5.4. On table 5.4, the WGS reactor is added in the system to convert CO into CO_2 and H_2. Therefore, hydrogen and carbon dioxide compositions are higher than its outlet from the reformer.

Table 5.3 The result of POX process at the standard condition

Molar flow of inlet stream (kmol/h)	
glycerol	1
oxygen	1.5
Inlet stream feed temperature (K)	273
System pressure (atm)	1
Partial oxidation reformer	
inlet temperature (K)	580
outlet temperature (K)	600
products composition (kmol/h)	
H_2	0.2580
CO_2	2.0575
CO	0.0094
CH_4	0.9331

Table 5.4 The result of POX process with WGS is added at the standard condition

Water gas shift reactor	
inlet temperature (K)	450
outlet temperature (K)	450
products composition (kmol/h)	
H_2	0.2667
CO_2	2.0662
CO	0.0007
CH_4	0.9331

5.2.1 Effect of reaction temperature

In this part, the partial oxidation is studied between 600 and 1200 K. At a fixed of O/G molar feed ratio, the amount of hydrogen and carbon monoxide generated increase with the increasing temperature as same as the steam reforming process until it reaches the highest H_2 production. And then the hydrogen yield decreases because the reverse water gas shift reaction occurs better than partial oxidation reaction. The CO_2 concentration also increases at low temperature but decreases at a higher temperature for convert CO_2 into CO in the shift reaction. The only carbon monoxide content rapidly increases from this reaction. However side reaction, methanation, deceases with increasing temperature. From the result, the hydrogen generated is lower than it produced from SR process. The quantity of H_2 has a little different from by-products component. For WGS is added in this process shown in Fig. 5.9, H_2 and CO_2 are also increase to reach the maximum hydrogen content and remain constant to the final temperature. The carbon monoxide content still increases from reverse water gas shift reaction in the reformer. Figs. 5.8 and 5.9 show the variation of the POX products with constant R_{pox} ratio of 1.5 at the operating temperature of 600-1200 K and atmospheric pressure.
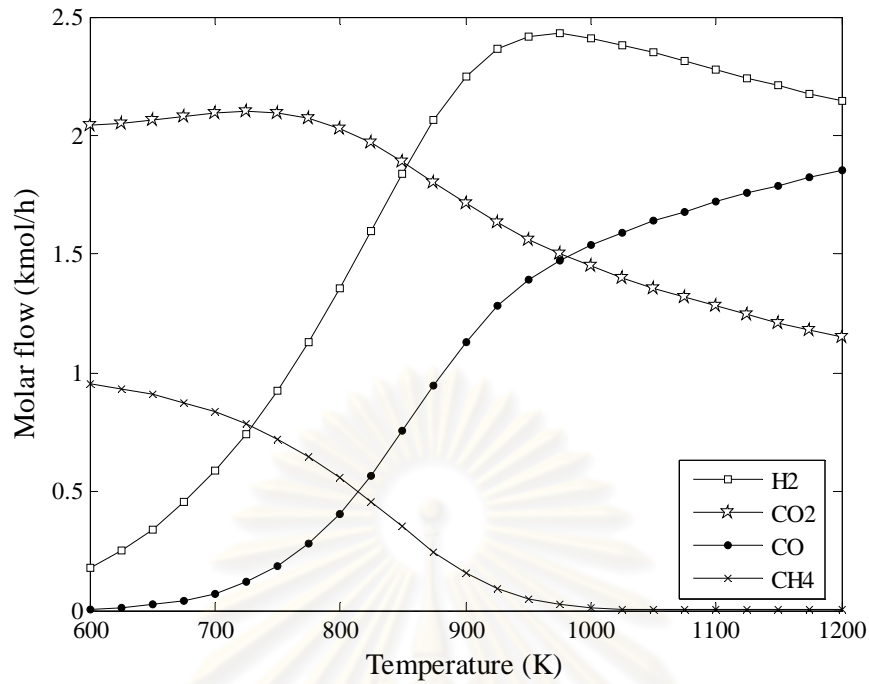
Fig. 5.8 Plot of thermodynamic equilibrium molar flow of each component based on O/G molar feed ratio of 1.5
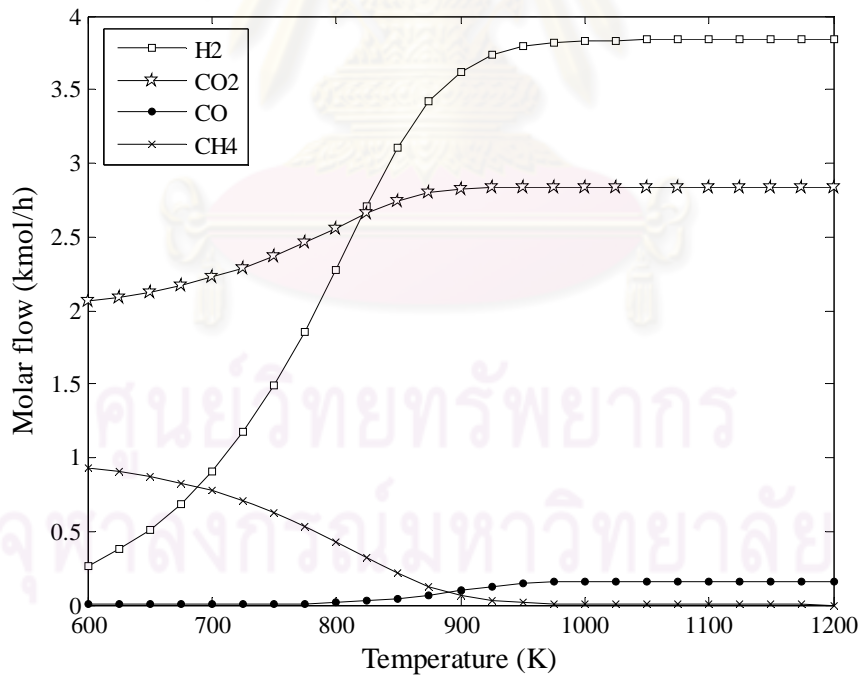
Fig. 5.9 Plot of thermodynamic equilibrium molar flow of each component based on O/G molar feed ratio of 1.5 which WGS is added

5.2.2 Effect of the oxygen-to-glycerol (O/G) molar feed ratio, R_{pox}

From the result, the hydrogen produced from WGS reactor is higher than reformer. Therefore, WGS reactor is added in this part to produce the maximum hydrogen content. The effect of varied R_{pox} ratio on hydrogen production is presented in Figs. 5.10-5.11. This result shows that the increasing of R_{pox} sharply increases the hydrogen production at the oxygen insufficient condition and slightly increases with O/G ratio higher than 1.5. At R_{pox} ratio higher than 3 makes the POX reaction occurs lower than reverse water gas shift reaction so that this work is not considered. Furthermore the amount of hydrogen is generated until it nearly constant in a higher range of R_{pox}. After the process reaches the maximum hydrogen yield, POX reaction is lower affected to this system. Meaning that, hydrogen molar flow is constant with increasing temperature higher than 1000 K. The result of O/G molar feed ratio, which is varied from 0.5 to 3, on the conversion of other components in Figs. 5.12-5.13 shows that all of the components are higher generated with increasing R_{pox} ratio. However, all of components have the same trend as H_2. Conversely, the concentration of CH_4 drops to zero at 950-980 K which is generated the maximum hydrogen. The maximum hydrogen yield of partial oxidation operation reaches only H_2-yield of 3.8 mole H_2/mole glycerol and is therefore much lower than the maximum reachable hydrogen yield from steam reforming, 7 mole H_2/mole glycerol, which WGS is added.
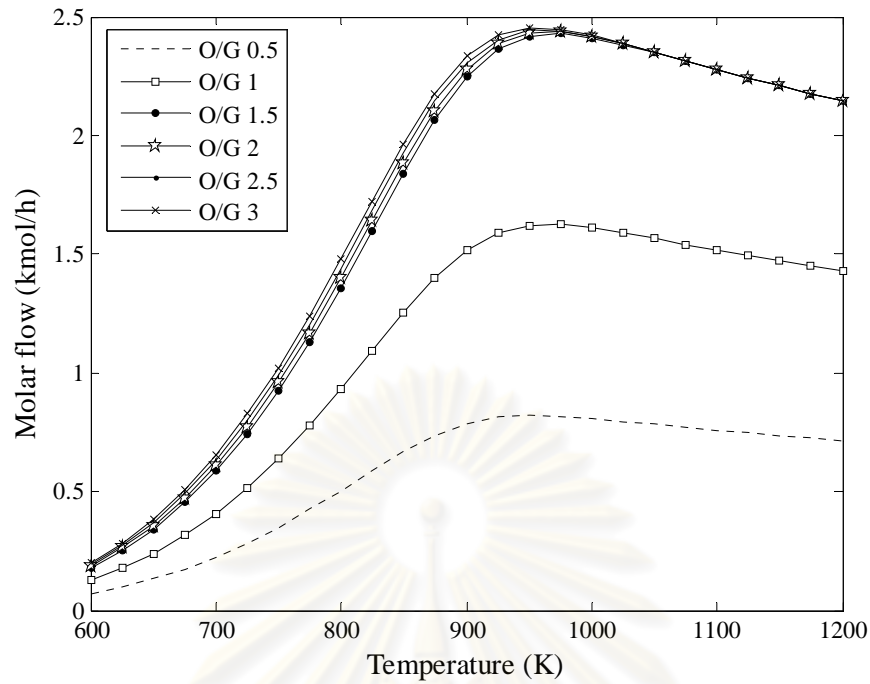
Fig. 5.10 Plot of thermodynamic equilibrium molar flow of hydrogen production at various ratios as a function of temperature when POX is employed
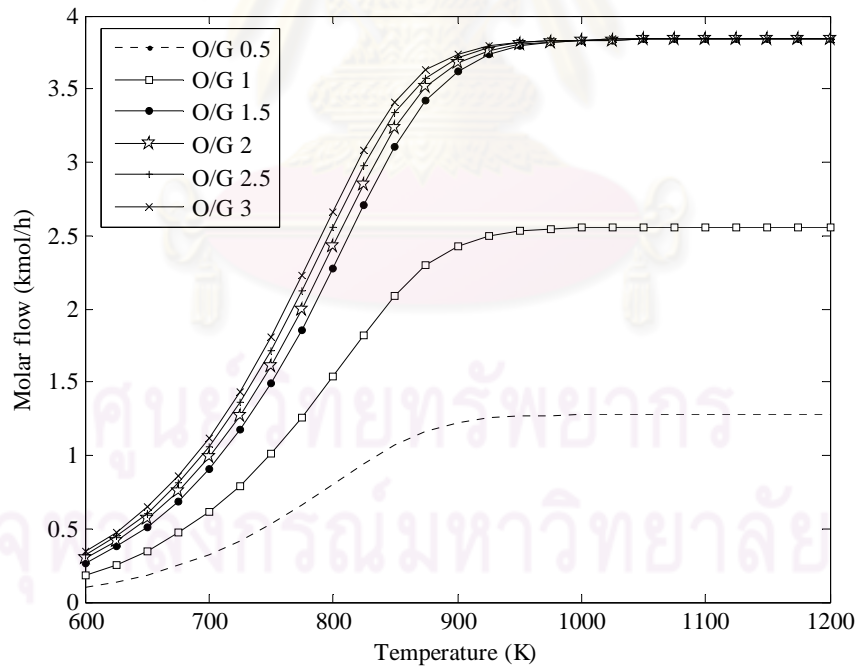
Fig. 5.11 Plot of thermodynamic equilibrium molar flow of hydrogen production at various ratios as a function of temperature which WGS is added when POX is employed
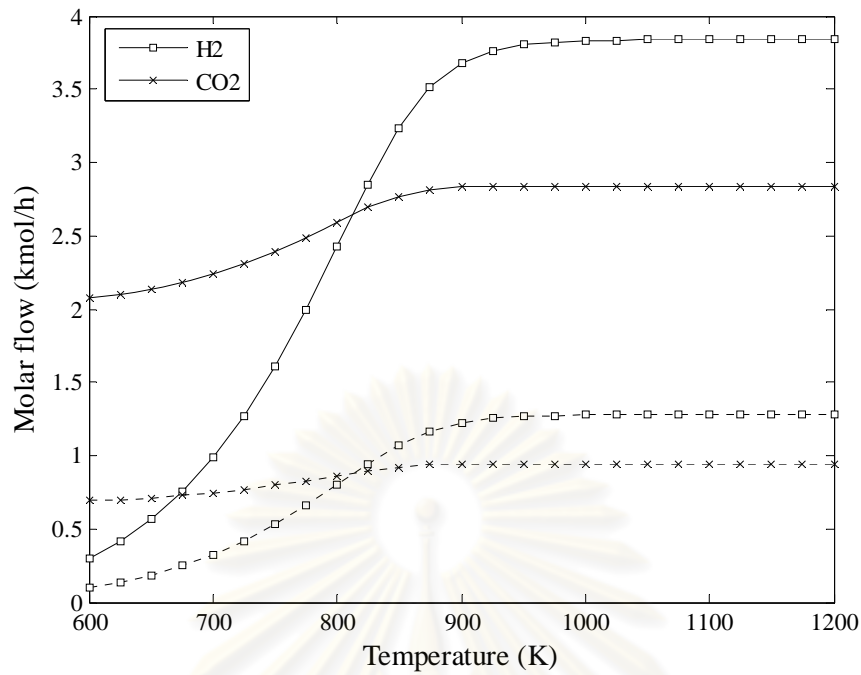
Fig. 5.12 Plot of thermodynamic equilibrium molar flow of hydrogen and carbon dioxide content at O/G molar ratio of 0.5 (dashed line) and 2 (solid line) as a function of temperature when POX is employed
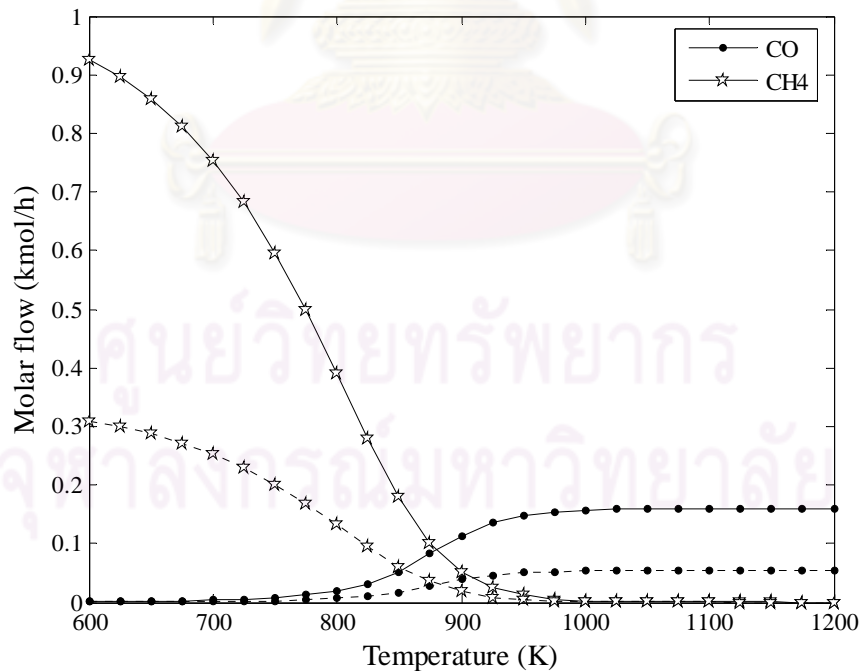
Fig. 5.13 Plot of thermodynamic equilibrium molar flow of carbon monoxide and methane content at O/G molar ratio of 0.5 (dashed line) and 2 (solid line) as a function of temperature when POX is employed

5.3 Autothermal reforming process for hydrogen production

   The effect of key parameters of autothermal reforming process i.e., S/G molar feed ratio (R_{sr}), O/G molar feed ratio (R_{pox}), preheating temperature at adiabatic condition and reaction temperature on the equilibrium compositions is studied and discussed in this part. At the standard condition, the R_{sr} ratio of 3, R_{pox} of 1.5 based on stoichiometric and reaction temperature at 600 K based on the minimum temperature that can be occurred are studied. The result at standard condition before parameters variation is shown in table 5.5. The WGS reactor is added in the system to convert CO into maximum hydrogen.

Table 5.5 The result of ATR process at the standard condition

Molar flow of inlet stream (kmol/h)	
glycerol	1
water	3
oxygen	1.5
Inlet stream feed temperature (K)	273
System pressure (atm)	1
Autothermal reformer	
inlet temperature (K)	580
outlet temperature (K)	600
WGS reactor	
products composition (kmol/h)	
H_2	0.4641
CO_2	2.1157
CO	0.0005
CH_4	0.8838

5.3.1 Effect of reaction temperature

   In this section, the reforming temperature is also studied between 600 and 1200 K. At a fixed of S/G molar feed ratio shown in Fig. 5.14, the amount of hydrogen and carbon dioxide generated from ATR process increase with the increasing temperature until it reaches the highest H_2 production. The CO concentration also equal to zero at all the range of temperature because CO is completely converted into CO_2 and H_2 in the shift

reactor. However, the methanation which is a side reaction from ATR process uses to produce methane as the same tendency as SR and POX system
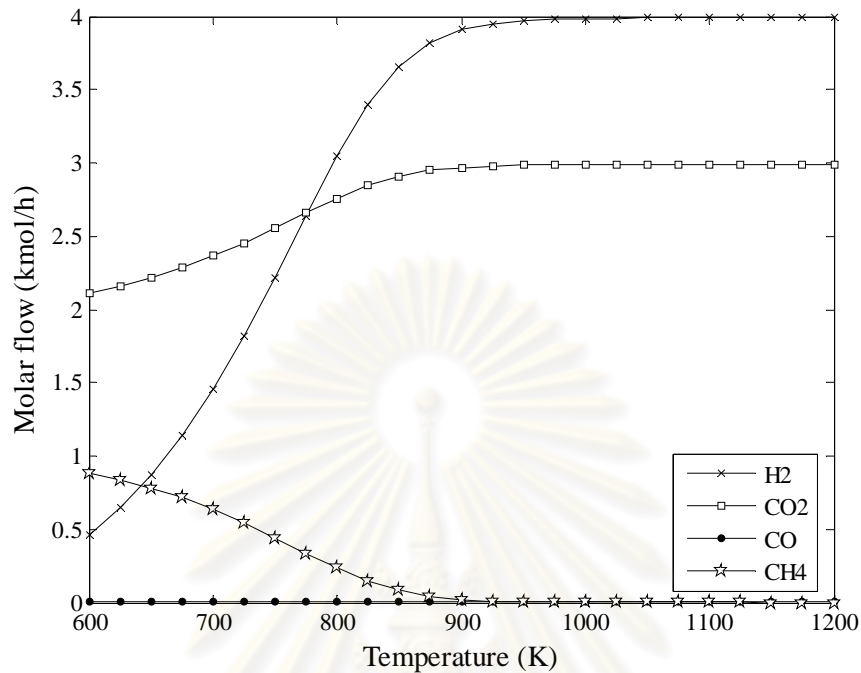
Fig. 5.14 Plot of thermodynamic equilibrium molar flow of each component based on S/G molar ratio of 3 and O/G molar ratio of 1.5 as a function of temperature

5.3.2 Effect of molar feed ratio (R_{sr} and R_{pox})

Fig. 5.15 shows that the quantity of hydrogen production depends on R_{pox} and reaction temperature. From the result, hydrogen is generated to the maximum and remains constant. On the other hand, the amount of H_2 decreases with increasing R_{pox} ratio because the partial oxidation occurs lower at a higher R_{pox} ratio. The effect of varied R_{sr} ratio which R_{pox} and reaction temperature is fixed on the product compositions from 1 to 9 is presented in Fig. 5.16. The tendency of hydrogen production is as same as it produced from SR process. Moreover, Fig 5.17 indicates that the SR reaction occurs better than POX reaction at low temperature. But POX reaction has higher performance at high temperature.
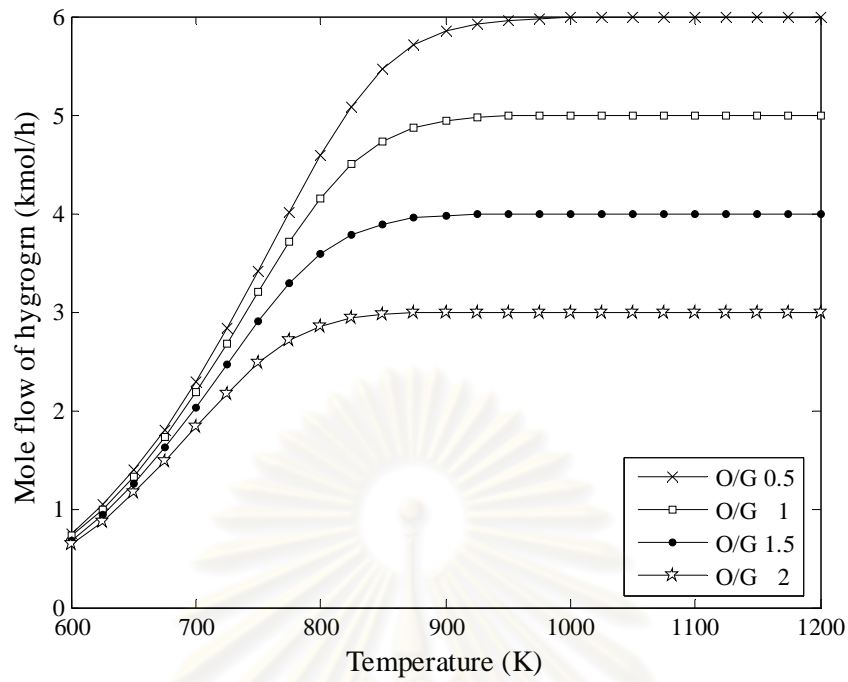
Fig. 5.15 Plot of thermodynamic equilibrium molar flow of hydrogen content at various R_{pox} ratios as a function of temperature which S/G ratio is fixed at 9
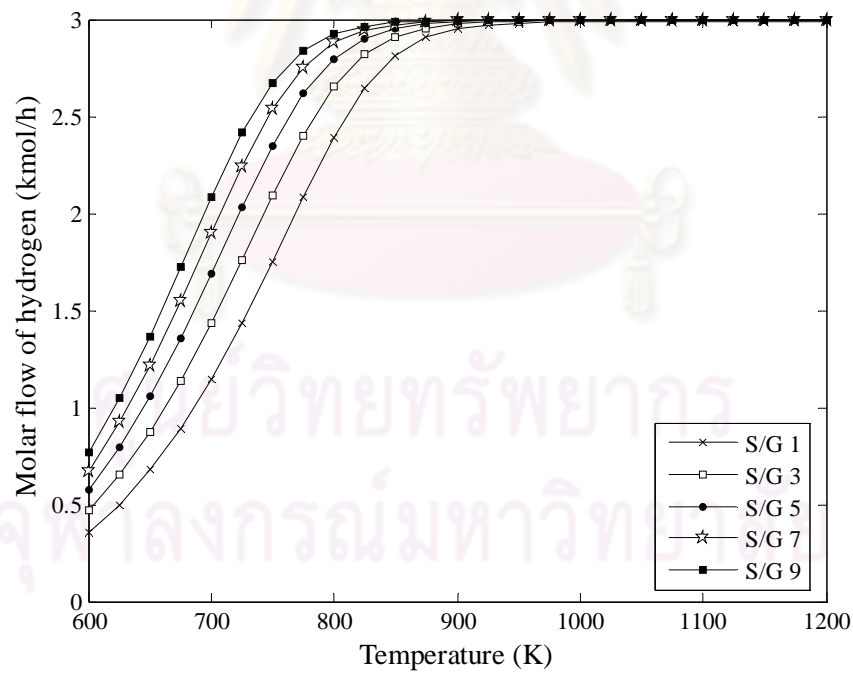
Fig. 5.16 Plot of thermodynamic equilibrium molar flow of hydrogen content at various R_{sr} ratios as a function of temperature which O/G ratio is fixed at 2
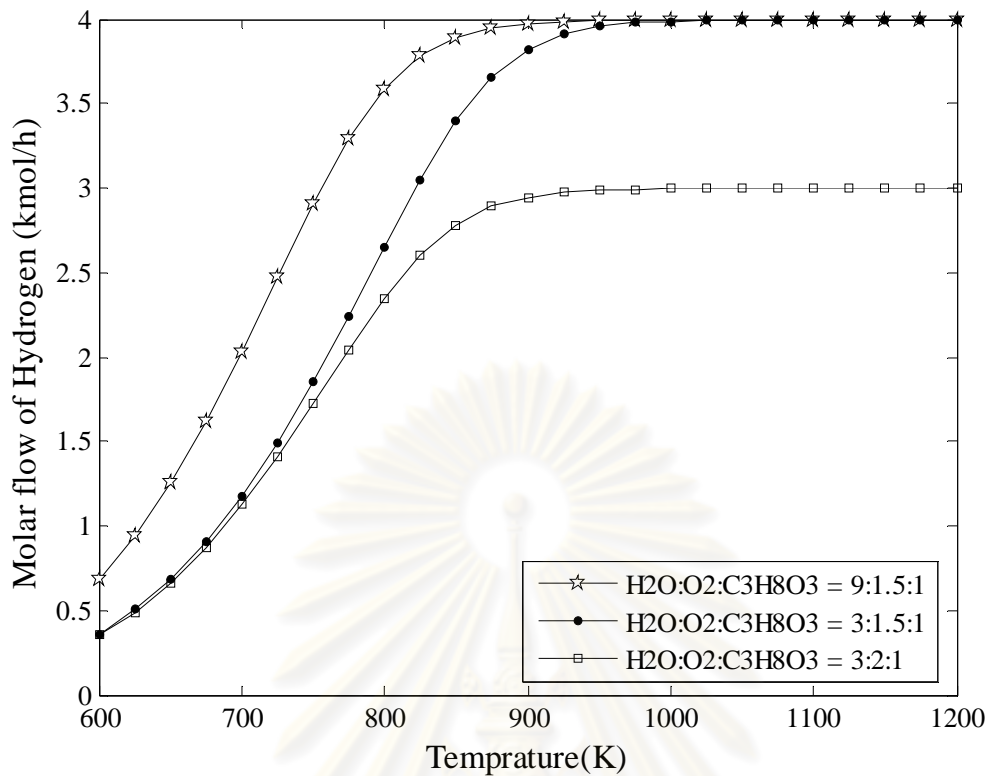
Fig. 5.17 Plot of thermodynamic equilibrium molar flow of hydrogen content at various R ratios as a function of temperature

To consider about the efficiency of reformer, gases production are simulated from the reformer. Fig. 5.18 shows the product components from ATR process which is varied R_{sr} ratios from 1 to 9 at 1100 K and O/G molar ratio of 2. Hydrogen and carbon dioxide are slightly generated with increasing R_{sr} ratio until it is nearly constant in a higher range of R_{sr}. However, CO concentration gradually decreases at higher R_{sr} ratio. Conversely, the effect of O/G molar feed ratio on the product compositions in ATR reactor at the constant temperature at 1100 K, S/G molar ratio of 9 and atmospheric pressure is presented in Fig. 5.19. The result shows that the amount of H_2 and CO has the same tendency. It decreases with increasing R_{pox} ratio. At higher R_{pox} ratio, POX reaction occurs better while SR reaction shifts to reverse reaction. Meaning that the content of hydrogen shapely decreases with increasing R_{pox} ratio. As same as the R-WGS reaction, CO concentration also decreases. Only CO_2 component increases from partial oxidation. The maximum hydrogen yield which is affected from POX reaction is 4 kmol/h.
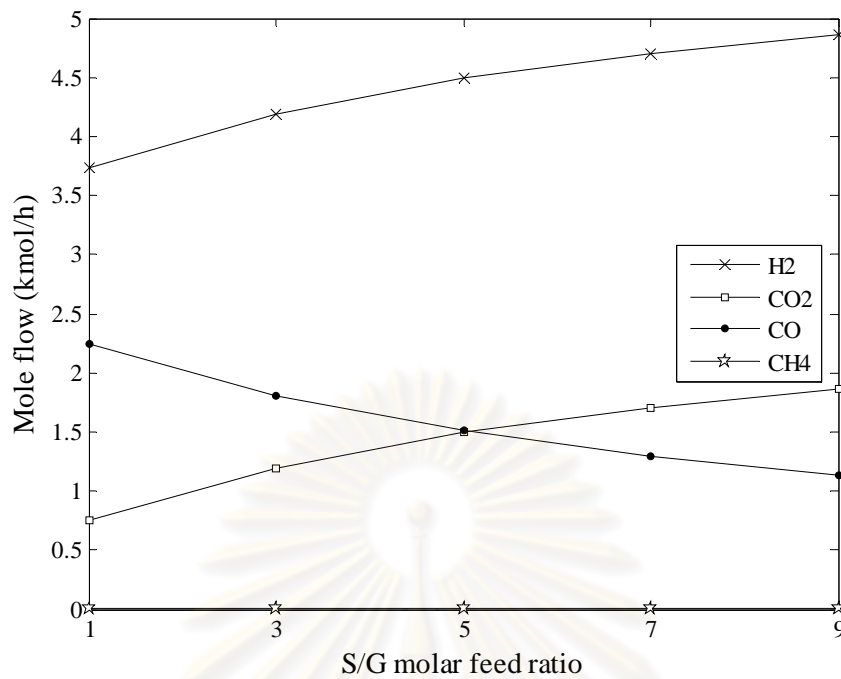
Fig. 5.18 Plot of thermodynamic equilibrium molar flow of the components at various R_{sr} ratios in ATR process at 1100 K, O/G molar ratio of 2 and atmospheric pressure
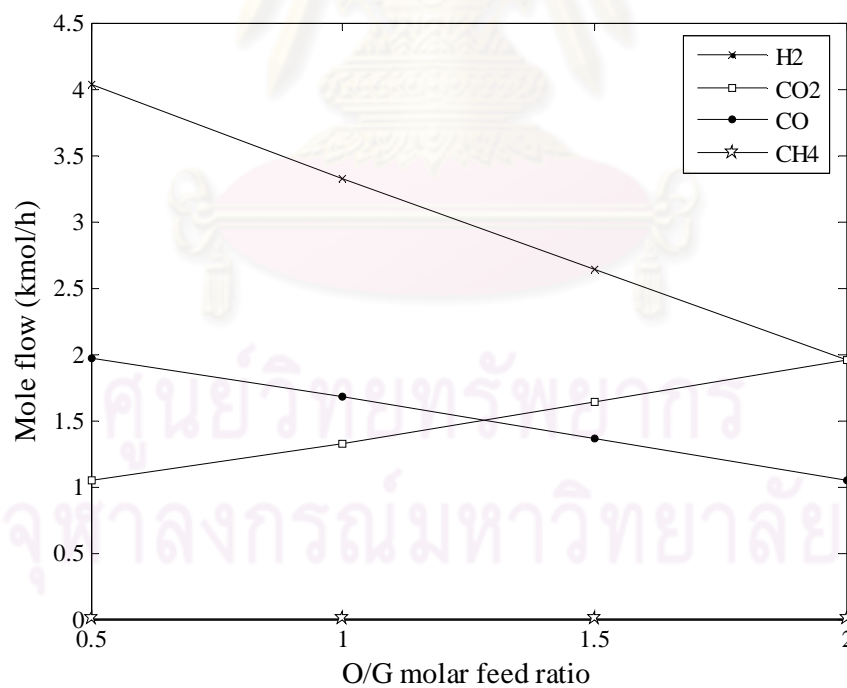
Fig. 5.19 Plot of thermodynamic equilibrium molar flow of the components at various R_{pox} ratios in ATR process at 1100 K, S/G molar ratio of 9 and atmospheric pressure

5.3.3 Effect of preheating temperature on adiabatic condition

From the result, Figs. 5.20-5.22 present the effect of preheating temperature on the product compositions in ATR process at the adiabatic condition, R_{pox} ratio of 0.5, R_{sr} ratio of 9 and atmospheric pressure. The result shows that the preheating temperature of 800 K gives a maximum hydrogen production. At this condition, the amount of CO_2, CO and CH_4 are the same tendency as it generated from reforming process. At the optimal preheating temperature, the system occurs at the reaction temperature of 905 K. At this condition, H_2, CO_2, CO and CH_4 are produced to 5.22, 2.30, 0.68 and 0.03 kmol/h, respectively.
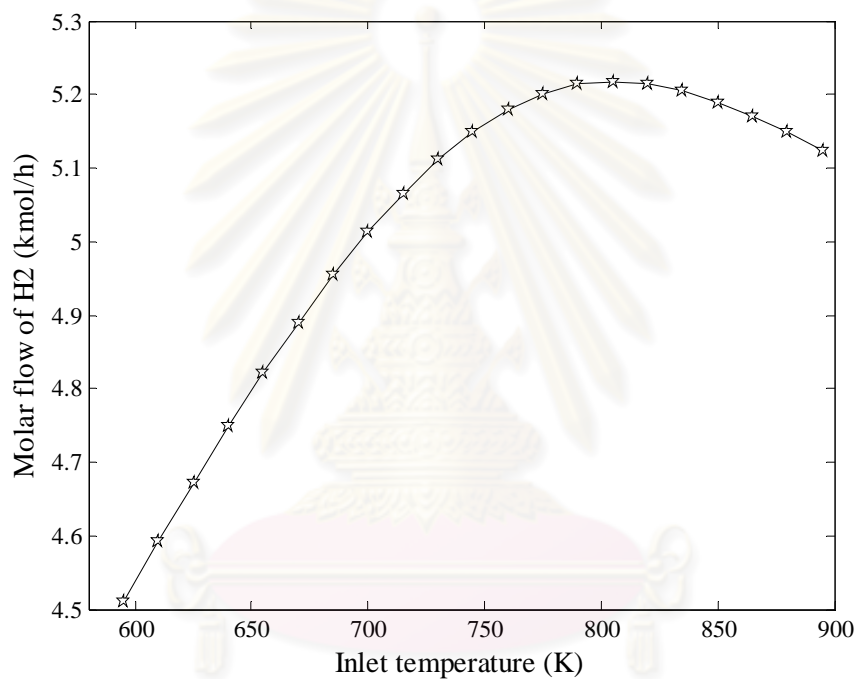
Fig. 5.20 Effect of preheating temperature on the hydrogen production in ATR reactor at the adiabatic condition, O/G ratio of 0.5, S/G ratio of 9 and atmospheric pressure
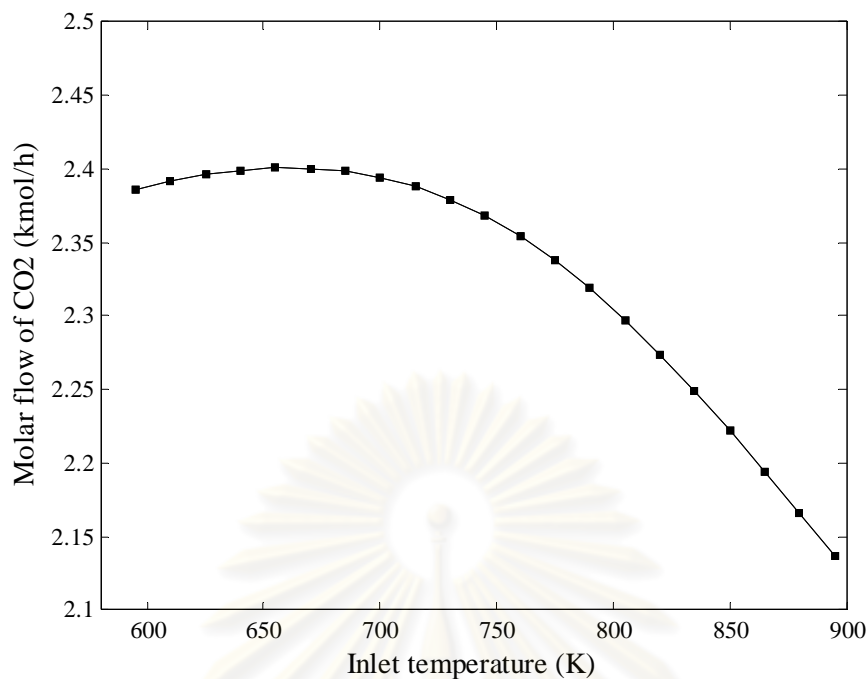
Fig. 5.21 Effect of preheating temperature on the CO_2 production in ATR reactor at the adiabatic condition, O/G ratio of 0.5, S/G ratio of 9 and atmospheric pressure
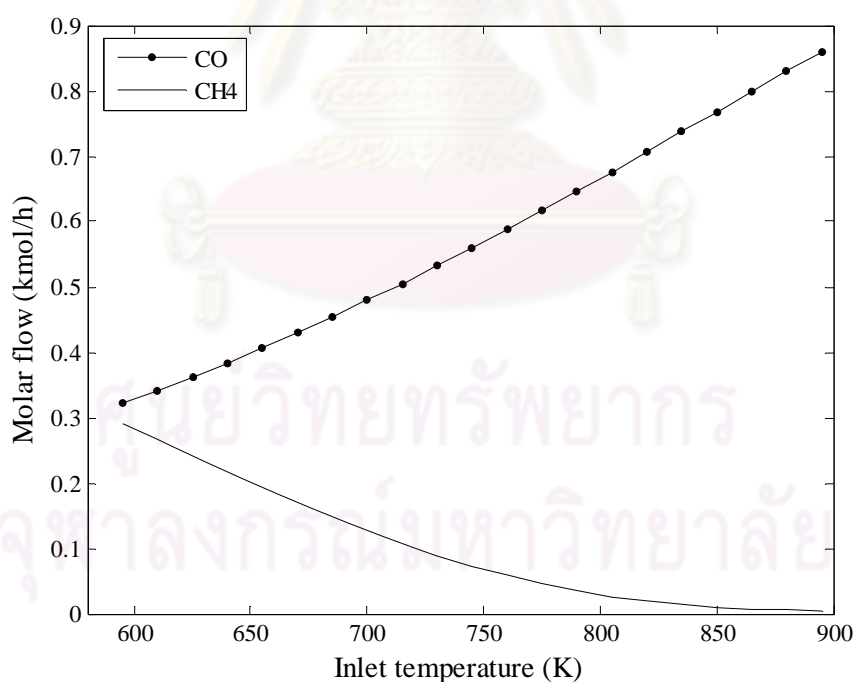
Fig. 5.22 Effect of preheating temperature on the CO and CH_4 production in ATR reactor at the adiabatic condition, O/G ratio of 0.5, S/G ratio of 9 and atmospheric pressure

5.4 Comparison between three processes, steam reforming, partial oxidation and autothermal reforming, for hydrogen production

This part is summary efficiency of the different reformer. To compare between SR and ATR process, from the result, all of the maximum hydrogen content produced from SR process is higher than ATR system at the constant temperature and pressure. At the maximum hydrogen yield, R_{sr} of 9, the steam reforming can be generated hydrogen upto 5.8 kmol/h but autothermal reforming produces less than 5 kmol/h. Meaning that POX reaction on ATR system reduces the efficiency of ATR reformer. But the CO component generated from ATR is lower than SR. To compare between POX and ATR process, H_2 production and purification produced from POX reformer is a little. In the case of the product distribution, the amount of hydrogen production is of the order POX<ATR < SR. The result is shown in Table 5.6.

Table 5.6 The summary of the production components from the reformer at the maximum hydrogen condition

	R ratio	Reforming temperature (K)	Purification of H_2 (%)	H_2 (kmol/h)	CO_2 (kmol/h)	CO (kmol/h)	CH_4 (kmol/h)
SR	9	925	37.53	5.9768	2.1471	0.7793	0.0735
POX	2	925	12.98	2.5606	1.6579	1.3097	0.0324
ATR S/O/G	9/0.5/1	1200	33.52	5.9936	2.9939	0.0061	0.000

5.5 Heat integration for hydrogen and synthesis gas production

The reforming products for the three different options, steam reforming, partial oxidation and autothermal reforming are analyzed. The process energy requirements for the reformer consist of the evaporation energy for heating up of feed gases from ambient to reformer temperature, the reforming energy at reformer temperature and cooling energy of products from reformer to 450 K and the energy for convert CO into CO_2 and H_2 in the water gas shift reactor. The process energy needed is related to the moles of hydrogen in the reformer effluent. Energy necessary for heating and cooling is almost equal, which means that in a well-designed reformer with heat integration little energy is lost for heating and cooling.

5.5.1 Heat integration from steam reforming process

Heat integration using in the reforming process is described in this part. For all cases of steam reforming process, the amount of heat rapidly decrease in the range of temperature of 600-900 K and slightly increase to 1200 K. The result is shown in Figs. 5.23 and 5.24. The energy demand is given as energy per mole hydrogen produced. At the temperature range between 600 and 800 K, the energy requirement is much more than the hydrogen production. Therefore the SR process needs a lot of energy.
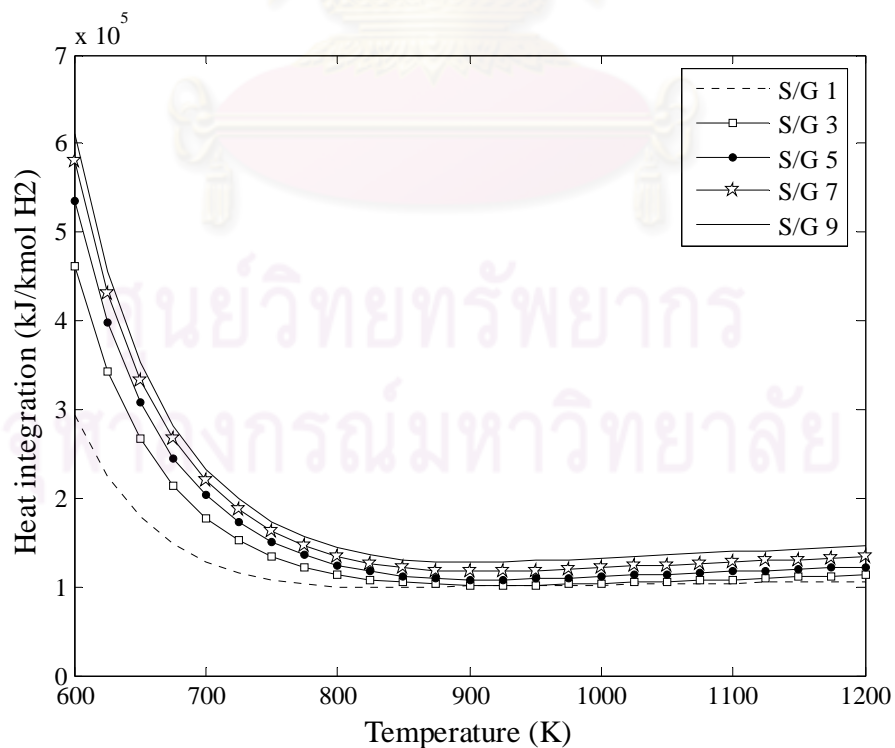
Fig. 5.23 Plot of heat integration from SR process for hydrogen production on thermodynamic equilibrium condition
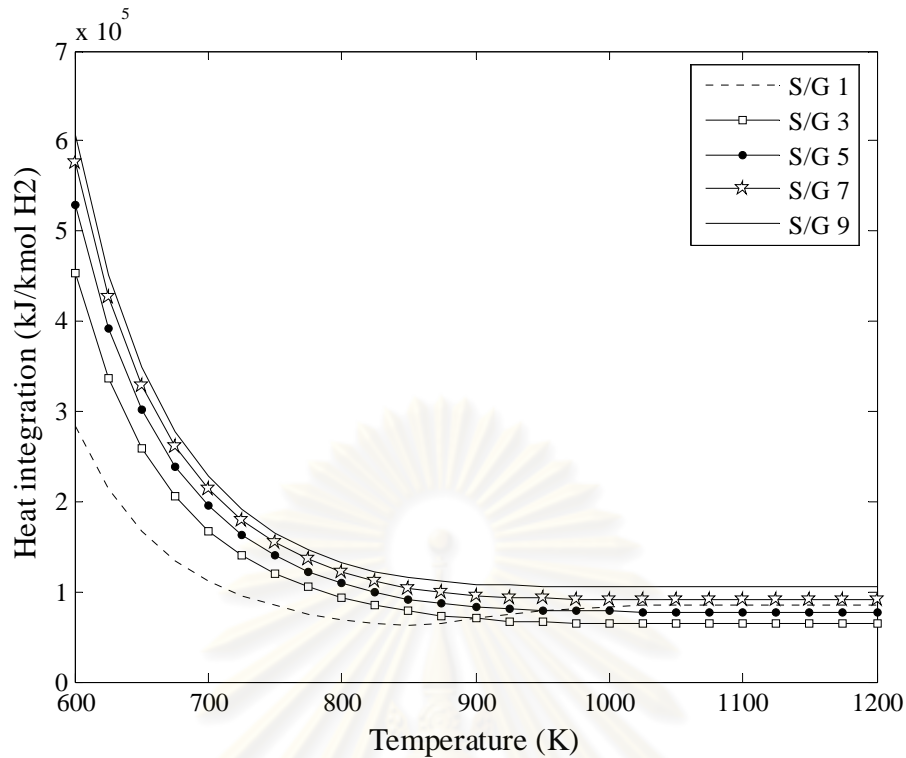
Fig. 5.24 Plot of heat integration from SR process for hydrogen production on thermodynamic equilibrium condition which WGS reactor is added

Table 5.7 presents total heat flow rate which depends on the ratio R_{sr} in each reactor. Because of the higher quantity of water, the energy demand on the evaporator increases with increasing R_{sr}. The energy demand of other reactors in term of R_{sr} ratio is slightly differed.

Table 5.7 Summary of the energy demand from each reactor in SR process at 1200 K for the maximum H_2 as a function of R_{sr} ratio

S/G	Evaporator $*10^5$ kJ/h	Reformer $*10^5$ kJ/h	Cooler $*10^5$ kJ/h	WGS reactor $*10^5$ kJ/h	Total heat flow $*10^5$ kJ/h
1	2.243	4.177	-1.861	-0.283	4.276
3	3.292	4.523	-2.458	-0.838	4.519
5	4.342	4.912	-3.047	-0.785	5.422
7	5.391	5.328	-3.630	-0.694	6.395
9	6.441	5.762	-4.210	-0.620	7.373

5.5.2 Heat integration from partial oxidation process

For all cases of partial oxidation process, the amount of heat sharply increases at the temperature lower than 900 K and remain constant to the final. The result is shown in Figs. 5.25 and 5.26. At the temperature range between 600 and 900 K before the maximum hydrogen generated, the energy requirement releases much more than the hydrogen which is produced. Therefore the POX process discharges a lot of energy. The maximum hydrogen is produced at 920 K and then the heat integration is also constant.
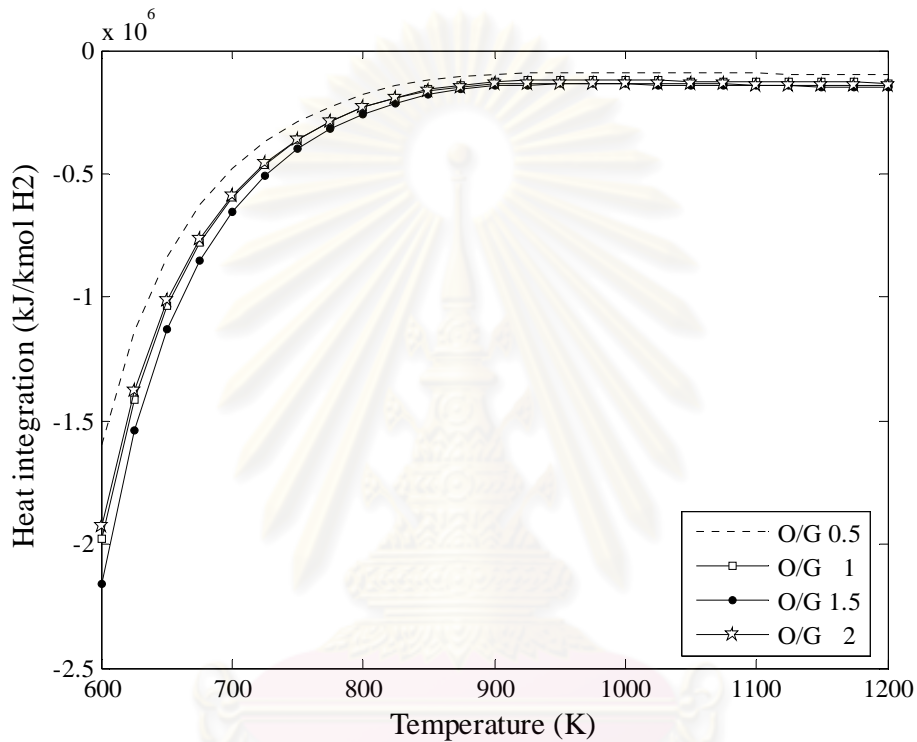
Fig. 5.25 Plot of heat integration from POX process for hydrogen production on thermodynamic equilibrium condition
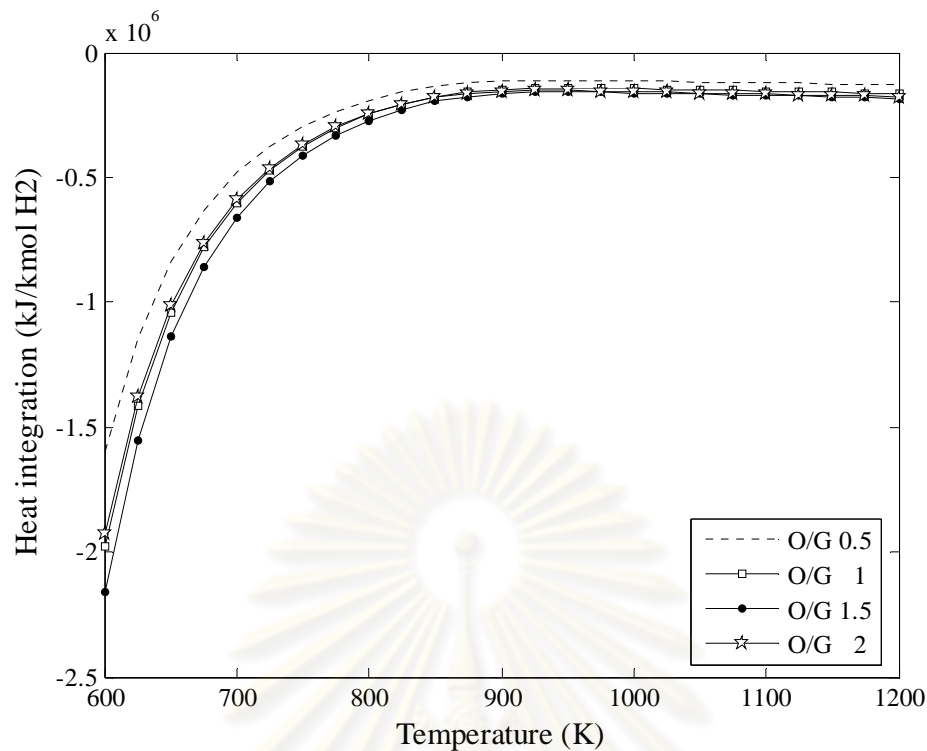
Fig. 5.26 Plot of heat integration from POX process for hydrogen production on thermodynamic equilibrium condition which WGS reactor is added

Table 5.8 presents total heat flow rate which depends on the ratio R_{pox} in each reactor. In this partial oxidation process, an exothermic process, a lot of heat depends on R_{pox} ratio is released from the reformer. However the energy demand of other reactors in term of R_{pox} ratio is slightly differed.

Table 5.8 Summary of the energy demand from each reactor in POX process at 920 K for the maximum H_2 as a function of R_{pox} ratio

O/G	Evaporator $*10^5$ kJ/h	Reformer $*10^5$ kJ/h	Cooler $*10^5$ kJ/h	WGS reactor $*10^5$ kJ/h	Total heat flow $*10^5$ kJ/h
0.5	1.671	-0.811	-1.638	-0.162	-0.940
1	1.821	-2.330	-1.555	-0.335	-2.399
1.5	2.265	-3.851	-1.897	-0.509	-3.992
2	2.445	-3.568	-2.233	-0.511	-3.867
2.5	2.623	-3.292	-2.568	-0.513	-3.741
3	2.805	-3.020	-2.903	-0.514	-3.632

5.5.3 Heat integration from autothermal reforming process

The energy needed for reforming shown in Fig. 5.27 is strongly reduced with increasing R_{sr} ratio in the temperature range of 600-800 K when operating in autothermal mode. On the other hand, increasing the R_{pox} ratio raises the energy demands at high temperature. Fig. 5.28 illustrates total heat integration which depends on the ratio R_{sr} in ATR process. And Table 5.9 presents total heat integration which depends on the ratio R_{sr} in each reactor. Because of the higher quantity of water, the energy demand on the evaporator increases with increasing R_{sr}. The energy demand of other reactors in term of R_{sr} ratio is slightly differed.
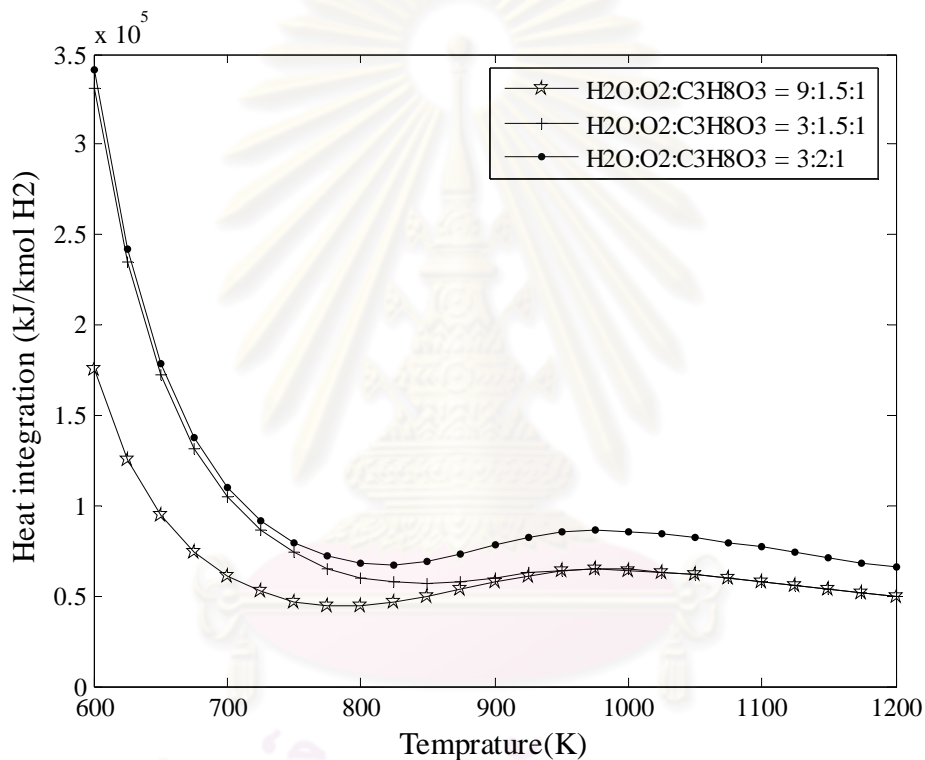
Fig. 5.27 Plot of heat integration for hydrogen production on thermodynamic equilibrium condition on autothermal reforming process
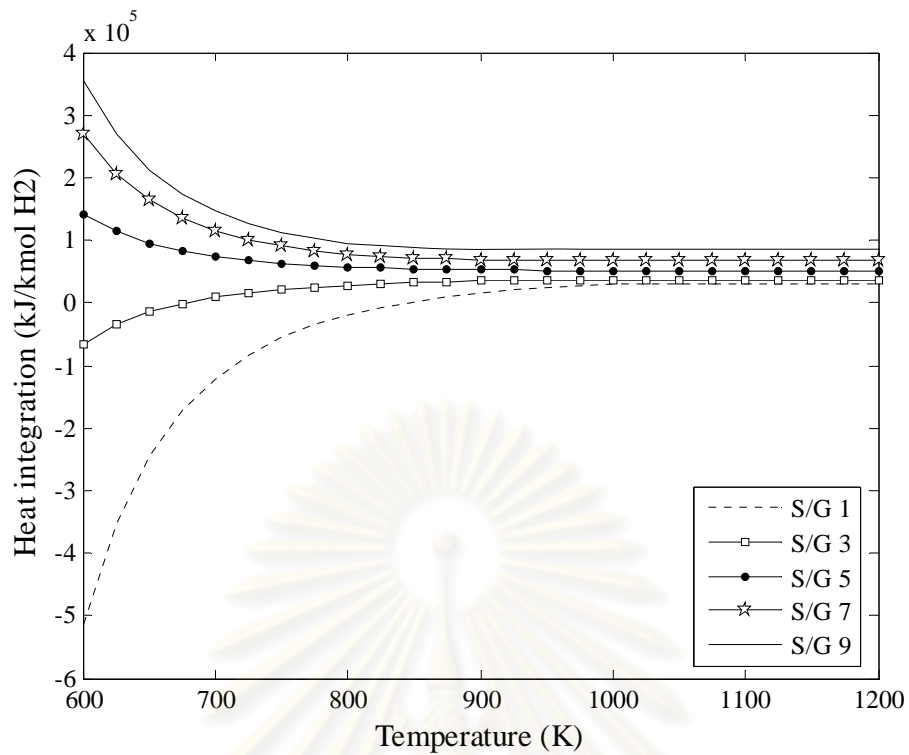
Fig. 5.28 Plot of heat integration for hydrogen production on thermodynamic equilibrium condition at various R_{sr} ratios and fixed R_{pox} at 0.5 in ATR process

Table 5.9 The amount of heat in each reactor on thermodynamic equilibrium condition at O/G ratio of 0.5, 1100 K and atmospheric pressure

S/G	Evaporator $*10^5$ kJ/h	Reformer $*10^5$ kJ/h	Cooler $*10^5$ kJ/h	WGS reactor $*10^5$ kJ/h	Total heat flow $*10^5$ kJ/h
1	2.426	1.672	-2.039	-0.501	1.558
3	3.475	1.931	-2.546	-0.729	2.131
5	4.524	2.237	-3.045	-0.617	3.099
7	5.573	2.572	-3.539	-0.531	4.075
9	6.623	2.926	-4.030	-0.466	5.053

When R_{sr} ratio is fixed at 9, the result is illustrated in Fig. 5.29 and Table 5.10. Total heat integration and heat flow rate in each reactor which depends on the R_{pox} ratio in ATR process is the same tendency. Because of the higher quantity of air inlet, a lot of heat depends on R_{pox} ratio is released from the reformer. The energy demand of other reactors in term of R_{pox} ratio is slightly differed.
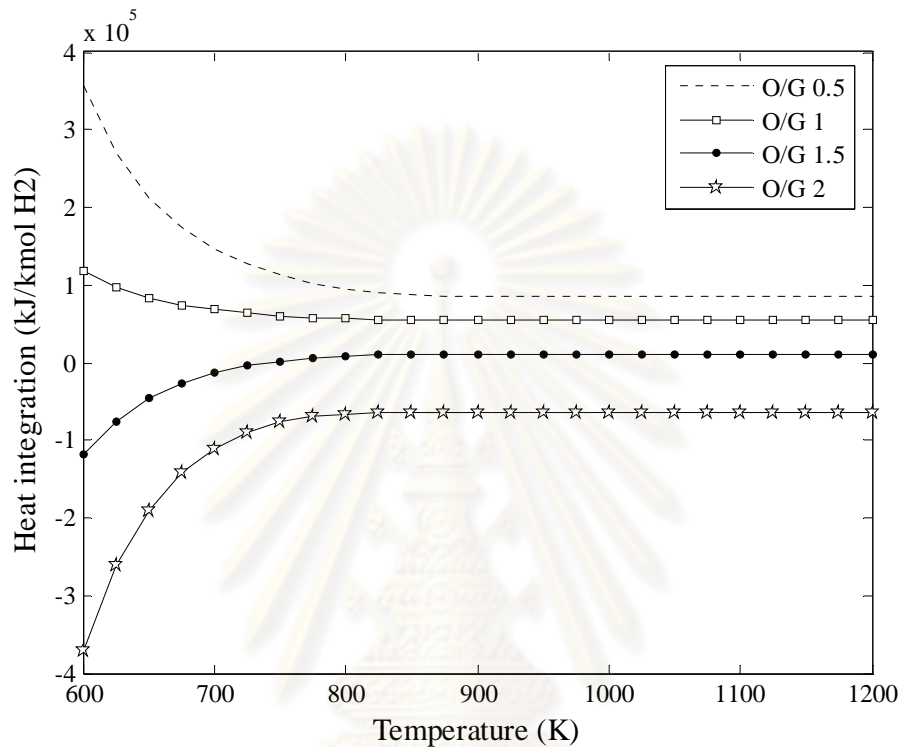
Fig. 5.29 Plot of heat integration for hydrogen production on thermodynamic equilibrium condition at various R_{pox} ratios and fixed R_{sr} at 9 in ATR process

Table 5.10 The amount of heat in each reactor on thermodynamic equilibrium condition at S/G ratio of 9, 1100 K and atmospheric pressure

O/G	Evaporator $*10^5$ kJ/h	Reformer $*10^5$ kJ/h	Cooler $*10^5$ kJ/h	WGS reactor $*10^5$ kJ/h	Total heat flow $*10^5$ kJ/h
0.5	6.623	2.926	-4.030	-0.466	5.053
1	6.805	0.783	-4.446	-0.388	2.754
1.5	6.988	-1.359	-4.900	-0.311	0.418
2	7.171	-3.501	-5.336	-0.234	-1.900

5.5.4 Comparison of the heat integration on each process

Fig. 5.30 and Table 5.11 show the different energy demands for steam reforming, partial oxidation and autothermal reforming process. The reasonable hydrogen yields are given at temperatures above 900 K. The largest amount of energy is necessary for evaporation and reforming. The comparison of steam reforming, partial oxidation and autothermal reforming in terms of energy demand is complicated, since in partial oxidation and autothermal, a part of the fuel is used for heat generation, which lowers the external energy demand. The operating condition of the result can be solved at the maximum hydrogen production. Steam reforming process generates at R_{sr} ratio of 9. Partial oxidation produced at R_{pox} ratio of 3. And autothermal reforming operates at R_{sr} and R_{pox} ratio of 9 and 0.5, respectively.
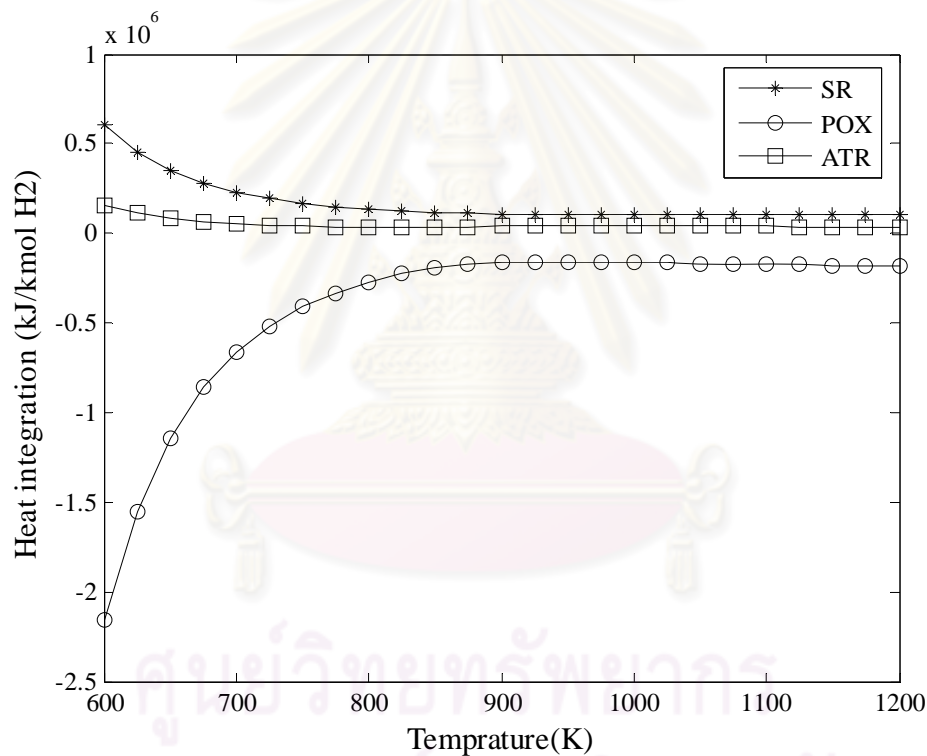
Fig 5.30 Plot of the heat integration for the maximum hydrogen condition with the different processes

Table 5.11 The amount of heat in each reactor from different process for the maximum hydrogen generated on thermodynamic equilibrium condition

Reformer	Evaporator $*10^5$ kJ/h	Reformer $*10^5$ kJ/h	Cooler $*10^5$ kJ/h	WGS reactor $*10^5$ kJ/h	Total heat flow $*10^5$ kJ/h
SR	6.441	5.762	-4.210	-0.620	7.373
POX	1.671	-0.811	-1.638	-0.162	-0.940
ATR	6.623	2.926	-4.030	-0.466	5.053

The result shows a complete different energy demand from three processes for the maximum hydrogen, whereas partial oxidation is the most energy demanding operation. This means from viewpoint of hydrogen content in the reformer effluent. The total energy demands that following order in terms of efficiency is steam reforming, autothermal and partial oxidation, respectively.

5.6 Optimization for different reforming processes

For each of the molar feed ratio (R_{sr} and R_{pox}), there is an optimal temperature for reformer operation to provide the maximum H_2 yield in the range of the reaction temperature between 600 and 1200 K. These data solving by HYSYS-Optimization are listed in Tables 5.12-5.15. Because this part considers the efficiency of the reformer, the products generated from the reformer are perused. Heat integration is a summary of energy demand which is given as energy per mole hydrogen produced from the process.

Table 5.12 The optimal operating temperature of glycerol steam reforming at various S/G ratios

S/G ratio	Optimum temperature (K)	H_2 concentration (kmol/h)	CO_2 concentration (kmol/h)	CO concentration (kmol/h)	Total heat flow ($*10^6$kJ/h)
1	1150	4.3208	0.3411	2.6521	4.2660
3	1020	4.9465	1.0375	1.9323	4.4567
5	950	5.3693	1.5868	1.3408	5.2972
7	930	5.8614	1.9952	0.9602	6.8076
9	900	5.9261	2.1473	0.7790	7.2465

Table 5.13 The optimal operating temperature of glycerol partial oxidation at various O/G ratios

O/G ratio	Optimum temperature (K)	H_2 concentration (kmol/h)	CO_2 concentration (kmol/h)	CO concentration (kmol/h)	Total heat flow ($*10^6$kJ/h)
0.5	930	0.8405	0.5297	0.4628	-0.9369
1	930	1.6728	1.0609	0.9207	-2.3933
1.5	930	2.5043	1.5924	1.3782	-3.9829
2	930	2.5243	1.5889	1.3898	-3.8593

Table 5.14 The optimal operating temperature of glycerol autothermal reforming various S/G ratios and fixed O/G ratio of 0.5

S/G ratio	Optimum temperature (K)	H_2 concentration (kmol/h)	CO_2 concentration (kmol/h)	CO concentration (kmol/h)	Total heat flow (*10^6kJ/h)
1	1050	3.7776	0.8147	2.1731	0.2354
3	1035	4.2975	1.3166	1.6773	0.3476
5	980	4.7219	1.7573	1.2311	0.4963
7	900	5.0070	2.1661	0.7811	0.6523
9	900	5.2172	2.3085	0.6613	0.7702

Table 5.15 The optimal operating temperature of glycerol autothermal reforming at various O/G ratios and fixed S/G ratio of 9

O/G ratio	Optimum temperature (K)	H_2 concentration (kmol/h)	CO_2 concentration (kmol/h)	CO concentration (kmol/h)	Total heat flow (*10^6kJ/h)
0.5	900	5.2172	2.3085	0.6613	0.7702
1	900	4.4192	2.4522	0.5369	1.0453
1.5	850	3.6136	2.6593	0.3254	1.3317
2	820	2.7638	2.7930	0.1973	1.6096

From the result, the optimization which is calculated by optimization program for the maximum hydrogen production closes to the data from solving by HYSYS simulation. Almost data is presented in appendix C. However, the result which is compared with the different reforming indicates that the optimal temperature for the maximum hydrogen produced is shift reverse from R_{sr} ratio. Meaning that, the maximum hydrogen yield can be generated at a lower temperature but higher R_{sr} ratio. At a higher R_{sr} ratio condition, H_2 and CO_2 compositions are increase but CO content is decrease. For higher hydrogen produced at higher R_{sr} ratio, the total heat integration is also increase. At higher feed ratio, the total energy demand is shapely increase but the different maximum hydrogen concentration is slightly increased.

The entire various R_{pox} ratio cases in the POX process, the maximum hydrogen is generated as the same optimum temperature. But the total production components are

increase with increasing R_{pox} ratio. Because POX is an exothermic process, the increasing of total heat integration which is released to the environment depends on R_{pox} ratio. At lower feed ratio than 0.5, the total energy released decreases and the purification of hydrogen at the maximum product condition also decreases too. The different of the product components, H_2, CO_2 and CO is a little.

The result from ATR process which is varied R_{sr} ratio and fixed R_{pox} ratio is as the same tendency as SR process. However, the maximum hydrogen and net energy demand of ATR is lower than SR process. In term of R_{pox} ratio, the maximum H_2 is as the same tendency as POX process, decreases hydrogen produced with increasing ratio, but the quantity from ATR is much more than POX system. For higher R_{pox} ratio, total heat integration of ATR is increase.

To summary of the optimum condition in term of reaction temperature, Steam reforming process should be generated at R_{sr} of 9 and the operating temperature of 900 K. Partial oxidation system should be operated at R_{pox} of 2 and the operating temperature of 930 K. And Autothermal reforming combined SR and POX process should be generated at R_{sr} of 9, R_{pox} of 0.5 and the operating temperature of 900 K.

CHARPTER VI

CONCLUSIONS

Three kinds of the thermodynamic equilibrium of glycerol steam reforming, partial oxidation and autothermal reforming by using HYSYS simulation software is discussed in this chapter. The main product set is hydrogen, carbon monoxide, carbon dioxide and methane. The number of moles of hydrogen produced is calculated based on equilibrium condition. The thermodynamic compositions are evaluated for S/G of 1–9 for SR and ATR process, O/G of 0.5–3 for POX process, O/G of 0.5–2 for ATR process and the reaction temperatures range between 600 and 1200 K.

In SR operation required a lot of heat to generated hydrogen, the study reveals that the best conditions for producing hydrogen is at the temperature higher than 900 K and a molar ratio of water to glycerol of 9:1. Under these conditions methane production is minimized. The upper limit of the moles of hydrogen produced per mole of glycerol is 5.98 in only reforming process and is 7 in WGS which is added versus the stoichiometric limit of 7. High temperatures and high R_{sr} favor the hydrogen production. Although water-rich feed increases the hydrogen production, a significant amount of unreacted water is resulted in the products. Because of the higher quantity of water, the energy demand on the evaporator increases with increasing R_{sr}. The energy demand of other reactors in term of R_{sr} ratio is slightly differed. Moreover, R-WGS reaction occurs better than SR reaction at high temperature.

In POX operation at which a lot of energy releases from the process, the study reveals that the best conditions for producing hydrogen is at the temperature of 930 K and a molar ratio of water to glycerol of 2:1. The upper limit of the moles of hydrogen produced per mole of glycerol is 2.52 versus the stoichiometric limit of 4. High temperatures favor the hydrogen production but decreases with higher R_{pox} ratio. In this operation, high hydrogen content appears in conjunction with high carbon monoxide content. At the temperature range between 600 and 900 K before the maximum hydrogen generated, the energy requirement releases much more than the hydrogen which is produced. Therefore the POX process discharges a lot of energy.

In ATR operation combined with steam reforming and partial-oxidation together, heat emission from POX reaction is used in SR reaction. The study reveals that the best

conditions for producing hydrogen is at the temperature of 900 K and a molar ratio of water:oxygen:glycerol of 9:0.5:1. At the constant temperature and pressure, POX reaction occurs better than SR reaction for all case.

Comparison of the above Figs. and Tables shows that the hydrogen content generated from glycerol steam reforming is the highest, followed by that created from autothermal reactions and by that produced from partial oxidation process. In cases of the total energy demand, which is the process energy for evaporation, reformation, and conversion of CO, the total energy demand is of the order POX<ATR < SR.

REFERENCES

Adhikaria, S.; Fernandoa S.; Gwaltneyb, S.R.; Toa, S.D.F.; Brickac, R.M.; Steeled, P.H.; and Haryantoa A. A thermodynamic analysis of hydrogen production by steam reforming of glycerol. International Journal of Hydrogen Energy 32 (2007): 2875 – 2880.

Alessandra, P. Hydrogen from ethanol: Theoretical optimization of a PEMFC system integrated with a steam reforming processor. International Journal of Hydrogen Energy 32 (2007): 1811 – 1819.

Akande, A.; Aboudheir, A.; Idem, R.; and Dalai, A. Kinetic modeling of hydrogen production by the catalytic reforming of crude ethanol over a co-precipitated Ni-Al_2O_3 catalyst in a packed bed tubular reactor. International Journal of Hydrogen Energy 31 (2006): 1707–1715.

Ariane, L.L.; Neuman, S.R.; Vera, M.M.S.; Jose, C.P. Modeling and optimization of the combined carbon dioxide reforming and partial oxidation of natural gas. Applied Catalysis A: General 215 (2001): 211–224.

Baocai, Z.; Xiaolan, T.; Yong, L.; Yide, X. and Wenjie, S. Hydrogen production from steam reforming of ethanol and glycerol over ceria-supported metal catalysts. International Journal of Hydrogen Energy 32 (2007): 2367 – 2373.

Benito, M.; Sanz, J.L.; Isabel, R.; Padilla R.; Arjona, R.; and Daza, L. Bio-ethanol steam reforming: Insights on the mechanism for hydrogen production. Journal of Power Sources 151 (2005): 11-17.

Costa, L.O.O.; Silva, A.M.; Borges, L.E.P.; Mattos, L.V. and Noronha, F.B. Partial oxidation of ethanol over Pd/CeO_2 and Pd/Y_2O_3 catalysts. Catalysis Today 138 (2008): 147-151.

Chaniotis, A.K.; Poulikakos, D. Modeling and optimization of catalytic partial oxidation methane reforming for fuel cells. Journal of Power Sources 142 (2005): 184–193.

Gerd, R. and Viktor, H. Hydrogen for fuel cells from ethanol by steam-reforming, partial-oxidation and combined auto-thermal reforming: A thermodynamic analysis. Journal of Power Sources 185 (2008): 1293-1304.

Giunta, P.; Mosquera, C.; Amadeo, N.; and Laborde, M. Simulation of a hydrogen production and purification system for a PEM fuel-cell using bioethanol as raw material. Journal of Power Sources 164 (2007): 336-343.

Hohn, K.L., and DuBois, T. Simulation of a fuel reforming system based on catalytic partial oxidation. Journal of Power Sources 183 (2008): 295-302.

Li, Y.; Wang, Y; Zhang, X.; and Mi, Z. Thermodynamic analysis of autothermal steam and CO_2 reforming of methane. International Journal of Hydrogen Energy 33 (2008): 2507–2514.

Lwin, Y.; Ramli, W.D.; Mohamad, A.B.; and Yaakob, Z. Hydrogen production from steam-methanol reforming: thermodynamic analysis. International Journal of Hydrogen Energy 25 (2000): 47–53.

Markovaa, D.; Bazbauers, G.; Valters, K.; Alhucema, A.R.; Weuffen, C.; and Rochlitz, L. Optimization of bio-ethanol autothermal reforming and carbon monoxide removal processes. Journal of Power Sources 193 (2009): 9–16.

Ni, M.; Leung, D.Y.C.; and Leung, M.K.H. A review on reforming bio-ethanol for hydrogen production. International Journal of Hydrogen Energy 32 (2007): 3238-3247.

Nianjun, L.; Fahai, C.; Xun, Z.; Tiancun, X. and Dingye, F. Thermodynamic analysis of aqueous-reforming of polylols for hydrogen generation. Fuel 86 (2007): 1727–1736.

Nianjun, L.; Xianwen, F.; Fahai, C.; Tiancun, X. and Peter, P.E. Glycerol aqueous phase reforming for hydrogen generation over Pt catalyst – Effect of catalyst composition and reaction conditions. Fuel 27 (2008): 3483–3489.

Nianjun, L.; Xun, Z.; Fahai, C.; Tiancun, X. and Dingye, F. Thermodynamic Study on Hydrogen Generation from Different Glycerol Reforming Processes. Energy & Fuels 21 (2007): 3505–3512.

Rodriguez, G. High Temperature Processes for Hydrogen Production. Hydrogen implementing Agreement (2006).

Song, S.J.; Kim, J.K.; Moon, J. H. and Lee, J.S. Thermodynamic optimization for coupled steam and oxidative reforming for hydrogen production. Journal of Ceramic Processing Research 9 (2008): 254-257.

Semelsberger, T.A.; Lee, F.B.; Rodney, L.B. and M.A.Michael, A.I. Equilibrium products from autothermal processes for generating hydrogen-rich fuel-cell feeds. International Journal of Hydrogen Energy 29 (2004): 1047-1064.

Seo, Y.S.; Shirley, A. and Kolaczkowski S. T. Evaluation of thermodynamically favourable operating conditions for production of hydrogen in three different reforming technologies. Journal of Power Sources 108 (2002): 213-225.

Shuhong, L.; Wenzhao, L.; Yuzhong, W. and Hengyong X. Catalytic partial oxidation of methane to syngas in a fixed-bed reactor with an O_2-distributor: The axial temperature profile and species profile study. Fuel Processing Technology 89 (2008): 1345-1350.

Sushil, A.; Sandun, F.; Steven, R.G.; Filip, T.; Mark, B.; Philip, H.S. and Agus H. A thermodynamic analysis of hydrogen production by steam reforming of glycerol. International Journal of Hydrogen Energy 32 (2007): 2875 – 2880.

Sushil, A.; Sandun, F. and Agus, H. A Comparative Thermodynamic and Experimental Analysis on Hydrogen Production by Steam Reforming of Glycerin. Energy & Fuels 21 (2007): 2306-2310.

Vagia, E.Ch. and Lemonidou A.A. Hydrogen production via steam reforming of bio-oil components over calcium aluminate supported nickel and noble metal catalysts. Applied Catalysis A: General 351 (2008): 111-121.

Wenju, W. and Yaquan, W. Thermodynamic analysis of hydrogen production via partial oxidation of ethanol. International Journal of Hydrogen Energy 33 (2008): 5035-5044.

Zahedi, N.M.; Rowshanzamir, S. and Eikani, M.H. Autothermal reforming of methane to synthesis gas: Modeling and simulation. International Journal of Hydrogen Energy 34 (2009): 1292-1300.

Zhixiang, L.; Zongqiang, M.; Jingming, X.U.; Natascha, H.M.; and Volkmar, M.S. Operation Conditions Optimization of Hydrogen Production by Propane Autothermal Reforming for PEMFC Application. Chinese J. Chem. Eng 14 (2006): 259-265.

APPENDICES
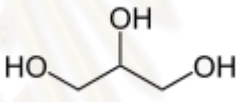
APPENDIX A

PHYSICAL PROPERTY

Glycerol

Glycerol is an organic compound, also called glycerin or glycerine. It is a colorless, odorless, viscous liquid that is widely used in pharmaceutical formulations. Glycerol has three hydrophilic hydroxyl groups that are responsible for its solubility in water and its hygroscopic nature. The glycerol substructure is a central component of many lipids. Glycerol is sweet-tasting and of low toxicity.

Table A.1 Glycerol property

Molecular formula	$C_3H_5(OH)_3$
Molecular structure	
Molar mass (g/mole)	92.09
Appearance	Clear, colorless
Density (g/ cm^3)	1.261
Melting point (˚C)	17.8
Boiling point (˚C)	290
Viscosity (Pa.S)	1.5
Solubility in water	Miscible

Air

Air is a mixture of gases especially oxygen required for breathing and which surrounds the earth.

Table A.2 Air property

Standard composition	
N$_2$	0.78
O$_2$	0.21
Ar	0.00038
Other gases	0.00962
Molar mass (g/mole)	28.95
Appearance	Clear, colorless
Gas density (kg/ m^3)	1.2 (at sea level)
Melting point (˚C)	-213.4
Boiling point (˚C)	-194.5
Viscosity (Pa.S)	$1.695 * 10^{-4}$

APPENDIX B

THERMODYNAMIC EQUILIBRIUM ANALYSIS

The relationship between the Gibbs energy and the equilibrium constant can be found by considering the chemical potentials. At constant temperature and pressure, the function G (Gibbs free energy) for the reaction depends only with the extent of reaction (ξ) and decrease according to the second law of thermodynamics. It means that the derivative of G with ξ must be negative. If the reaction happens at the equilibrium the derivative will be equal to zero.

$$\left(\frac{dG}{d\xi}\right)_{T,P} = 0 \tag{B.1}$$

The equilibrium system can be written as

$$\alpha A + \beta B \Leftrightarrow \sigma S + \tau T \tag{B.2}$$

In order to reach the thermodynamic equilibrium condition, the Gibbs energy must be stationary meaning that the derivative of G with respect to the extent of reaction, ξ, must be zero. It can be shown that in this case, the sum of chemical potentials of the products is equal to the sum of chemical potentials of the reactants. Therefore, the sum of the Gibbs energy of the products must be the equal to the sum of the Gibbs energy of the reactants.

$$\alpha\mu_A + \beta\mu_B = \sigma\mu_S + \tau\mu_T \tag{B.3}$$

μ is a partial molar Gibbs energy; a chemical potential.

The chemical potential of a reagent A is a function of the activity { A } of that reagent.

$$\mu_A = \mu_A^\ominus + RT \ln\{A\} \tag{B.4}$$

$\mu_A^\ominus$ is the standard chemical potential.

Substituting expressions like this into the Gibbs energy equation:

$$dG = VdP - SdT + \sum_{i=1}^{k} \mu_i dN_i \tag{B.5}$$

In the case of a closed system:

$$dN_i = \nu_i d\xi \tag{B.6}$$

v_i corresponds to the stoichiometric coefficient and $d\xi$ is the differential of the extent of reaction.

At constant pressure and temperature is obtained:

$$\left(\frac{dG}{d\xi}\right)_{T,p} = \sum_{i=1}^{k} \mu_i v_i = \Delta G_{T,P} \tag{B.7}$$

Results in

$$\Delta G_{T,P} = \sigma\mu_s + \tau\mu_T - \alpha\mu_A - \beta\mu_B \tag{B.8}$$

By substituting the chemical potentials:

$$\Delta G_{T,P} = \left(\sigma\mu_S^\Theta + \tau\mu_T^\Theta\right) - \left(\alpha\mu_A^\Theta + \beta\mu_B^\Theta\right) + \left(\sigma RT\ln\{S\} + \tau RT\ln\{T\}\right) - \left(\alpha RT\ln\{A\} + \beta RT\ln\{B\}\right) \tag{B.9}$$

The relationship becomes:

$$\Delta G_{T,P} = \sum_{i=1}^{k} \mu_i^\Theta v_i + RT\ln\frac{\{S\}^\sigma \{T\}^\tau}{\{A\}^\alpha \{B\}^\beta} \tag{B.10}$$

And

$$\sum_{i=1}^{k} \mu_i^\Theta v_i = \Delta G^\Theta \tag{B.11}$$

which is the standard Gibbs energy change for the reaction. It is a constant at a given temperature, which can be calculated, using thermodynamical tables.

$$RT\ln\frac{\{S\}^\sigma \{T\}^\tau}{\{A\}^\alpha \{B\}^\beta} = RT\ln Q_r \tag{B.12}$$

Q_r is the reaction quotient when the system is not at equilibrium.

Therefore:

$$\left(\frac{dG}{d\xi}\right)_{T,P} = \Delta G_{T,P} = \Delta G^\Theta + RT\ln Q_r \tag{B.13}$$

At the equilibrium condition:

$$\left(\frac{dG}{d\xi}\right)_{T,P} = \Delta G_{T,P} = 0 \tag{B.14}$$

$Q_r = K_{eq}$, the reaction quotient becomes equal to the equilibrium constant.

Then

$$0 = \Delta G^{\Theta} + RT \ln K_{eq} \qquad (B.15)$$

And

$$\Delta G^{\Theta} = -RT \ln K_{eq} \qquad (B.16)$$

Obtaining the value of the standard Gibbs energy change, allows the calculation of the equilibrium constant

Addition of reactants and products

For a reaction system at equilibrium:

$$Q_r = K_{eq} \text{ and } \xi = \xi_{eq} \qquad (B.17)$$

If the system is modified activities of constituents, the value of the reaction quotient changes and becomes different from the equilibrium constant:

$$Q_r \neq K_{eq} \qquad (B.18)$$

So that:

$$\left(\frac{dG}{d\xi} \right)_{T,P} = \Delta G^{\Theta} + RT \ln Q_r \qquad (B.19)$$

And from Eq. C.14

$$\Delta G^{\Theta} = -RT \ln K_{eq} \qquad (B.20)$$

Then

$$\left(\frac{dG}{d\xi} \right)_{T,P} = RT \ln \left(\frac{Q_r}{K_{eq}} \right) \qquad (B.21)$$

This can be divided into two cases:

- If the activity of reagent i increases, the reaction quotient decreases.

$$Q_r = \frac{\Pi(a_j)^{v_j}}{\Pi(a_i)^{v_i}} \qquad (B.22)$$

Then

$$Q_r < K_{eq} \text{ and } \left(\frac{dG}{d\xi} \right)_{T,P} < 0 \qquad (B.23)$$

Meaning that, the reaction will shift to the right, the forward direction, thus the process will form more products.

- If the activity of product j increases, the reaction quotient also increases. Then

$$Q_r > K_{eq} \text{ and } \left(\frac{dG}{d\xi}\right)_{T,P} > 0 \qquad (B.24)$$

Meaning that, the reaction will shift to the left, the reverse direction, and thus the process will form fewer products.
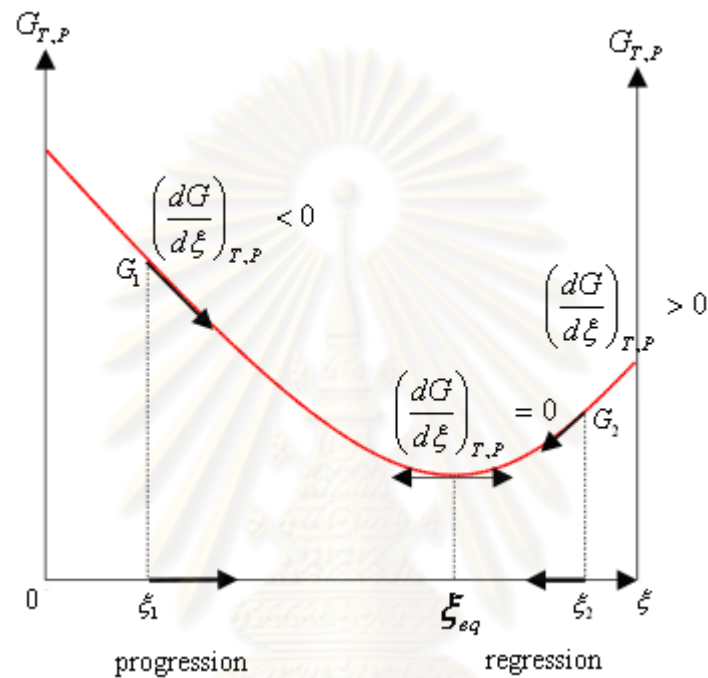

Fig. C.1 Plot the relationship between $G_{(T,P)}$ and $f(\xi)$

APPENDIX C

THE RESULTS OF THE OPTIMAZATION ANALYSIS

Table C.1 The optimal operating temperature of glycerol steam reforming at the different range of S/G ratio

S/G ratio	1	3	5	7	9
Opt. Temp.	1150	1020	950	930	900
Composition (kmol/h)					
H_2	4.3208	4.9465	5.3694	5.8614	5.9262
CO_2	0.3412	1.0375	1.5868	1.9953	2.1474
CO	2.6522	1.9323	1.3408	0.9603	0.7790
CH_4	0.0067	0.0302	0.0724	0.0445	0.0736
Energy demand ($*10^5$ kJ/h)					
Qevap	2.2431	3.29204	4.3412	5.9149	6.4399
Qsr	4.0210	3.7090	3.4500	3.6777	3.5103
Qcool	1.7257	1.8214	1.9492	2.3923	2.3852
Qwgs	-0.7272	-0.7229	-0.5444	-0.3926	-0.3185
sumQ	4.2659	4.4567	5.2972	6.8076	7.2465

TableC.2 The optimal operating temperature of glycerol partial oxidation process at the different range of O/G ratio

O/G ratio	0.5	1	1.5	2
Opt. Temp.	930	930	930	930
Composition (kmol/h)				
H_2	0.8405	1.6729	2.5043	2.5243
CO_2	0.5297	1.0610	1.5924	1.5887
CO	0.4628	0.9208	1.3782	1.3899
CH_4	0.0075	0.0183	0.0294	0.0215
Energy demand ($*10^5$ kJ/h)				
Qevap	1.6705	1.8205	2.2653	2.4453
Qpox	-0.7909	-2.3019	-3.8136	-3.5291
Qcool	1.6529	1.5737	1.9199	2.2589
Qwgs	-0.1636	-0.3382	-0.5146	-0.5165
sumQ	-0.9369	-2.3933	-3.9829	-3.8592

Table C.3 The optimal operating temperature f glycerol autothermal reforming process at the different R ratio

S: O: G	1: 0.5: 1	1: 1: 1	1: 1.5: 1	1: 2: 1	3: 0.5: 1	3: 1: 1	3: 1.5: 1	3: 2: 1	5: 0.5: 1	5: 1: 1	5: 1.5: 1	5: 2: 1
Opt. Temp.	1050	975	930	850	1035	930	900	850	980	900	900	820
Composition (kmol/h)												
H_2	3.7776	3.2841	2.7736	2.2128	4.2975	3.7727	3.1461	2.4726	4.7219	4.0803	3.3553	2.6013
CO_2	0.8147	1.3475	1.8298	2.3461	1.3166	1.8652	2.2074	2.5359	1.7573	2.1854	2.3862	2.6847
CO	2.1731	1.6315	1.1515	0.6094	1.6773	1.1040	0.7721	0.4429	1.2311	0.7796	0.6035	0.2874
CH_4	0.0122	0.0211	0.0187	0.0445	0.0061	0.0308	0.0204	0.0212	0.0116	0.0350	0.0103	0.0279
Energy demand ($*10^5$ kJ/h)												
Qevap	2.4260	2.6079	2.7896	2.9716	3.4746	3.6567	3.8387	4.0208	4.5236	4.7059	4.8881	5.0704
Qsr	1.8678	1.9669	2.1011	1.9719	2.2694	2.1402	2.2850	2.2570	2.4333	2.3186	2.6093	2.3230
Qcool	-0.4850	-0.6083	-0.4648	-0.2477	-0.6763	-0.4491	-0.3150	-0.1807	-0.5026	-0.3184	-0.2468	-0.1172
Qwgs	1.4546	-1.1837	-3.7430	-6.6393	1.5916	-1.3149	-3.7892	-6.4540	1.4915	-1.3483	-3.5881	-6.5348
sumQ	2.3541	5.1501	8.1689	11.3351	3.4760	6.6628	9.5979	12.5511	4.9627	8.0544	10.8387	13.8110

Table C.3 The optimal operating temperature of glycerol autothermal reforming process at the different R ratio (continue)

S: O: G	7: 0.5: 1	7: 1: 1	7: 1.5: 1	7: 2: 1	9: 0.5: 1	9: 1: 1	9: 1.5: 1	9: 2: 1
Opt. Temp.	900	900	850	820	900	900	850	820
Composition (kmol/h)								
H_2	5.0070	4.2864	3.5113	2.7014	5.2172	4.4192	3.6136	2.7638
CO_2	2.1661	2.3432	2.5876	2.7494	2.3085	2.4522	2.6593	2.7930
CO	0.7811	0.6379	0.3870	0.2346	0.6613	0.5369	0.3254	0.1973
CH_4	0.0528	0.0189	0.0254	0.0160	0.0302	0.0110	0.0152	0.0098
Energy demand ($*10^5$ kJ/h)								
Qevap	5.5730	5.7552	5.9377	6.1201	6.6223	6.8047	6.9873	7.1698
Qsr	2.3522	2.6427	2.5660	2.5789	2.6764	2.9642	2.8459	2.8337
Qcool	-0.3192	-0.2609	-0.1581	-0.0957	-0.2705	-0.2198	-0.1331	-0.0805
Qwgs	1.0835	-1.1261	-3.8177	-6.3518	1.3258	-0.9040	-3.6170	-6.1730
sumQ	6.5225	9.2632	12.1633	14.9550	7.7022	10.4532	13.3172	16.0960

APPENDIX D

HYSYS SIMULATION PROGRAM

In this work, different reforming processes for the production of hydrogen from glycerol obtained from biodiesel production was studied by using Hysys simulation software (Fig. D.1). The reforming processes of glycerol including steam reforming, partial oxidation and autothermal reforming consist of an evaporator, a reformer and a water gas shift reactor. The temperature and pressure of glycerol, water and air feeds are fixed at 273 K and 1 atm, respectively. The evaporator is employed to vaporize glycerol and water in liquid phase to the temperature of 580 K. The different reformers generate synthesis gas, H_2 and CO, at the temperature range between 600 and 1200 K. The synthesis gas is cooled down to 450 K before entering the WGS reactor. Because of the limitation of heat transfer in heat exchangers, the gaseous products from the reformer are first cooled-down into 480 K by preheating a glycerol feed. This reduces the energy demand of the evaporator. Because fuel cell electrodes can tolerate only very low concentrations of carbon monoxide at low temperature, the water gas shift reactor is added to remove CO from the synthesis gas.
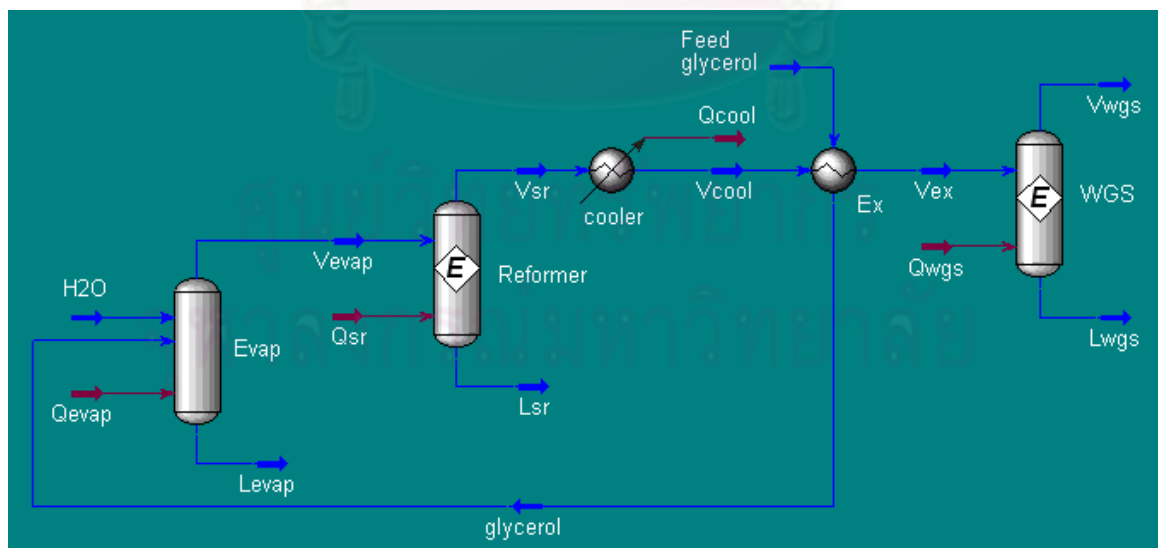

Fig. D.1 Reforming process of glycerol

To perform an opimizaton in Hysys, the first step is to set up an objective function. In this study, the objective is to maximize hydrogen production from the reforming process of glycerol (Fig. D.2). Then, all important variables used to solve the optimization problem are selected as shown in Fig. D.3. The outlet temperature of the reformer is selected as an optimization variable in this work. It is noted that product components are employed to evaluate the reformer performance in terms of the production and purification of hydrogen. Total heat requirement is another choice to consider the reformer efficiency.
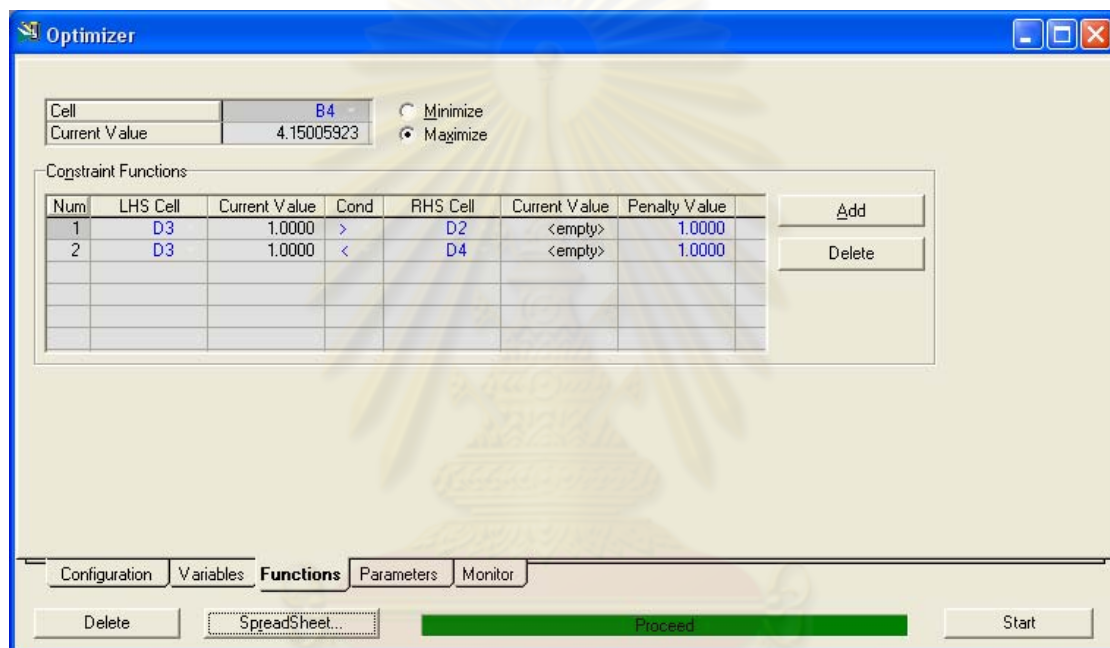

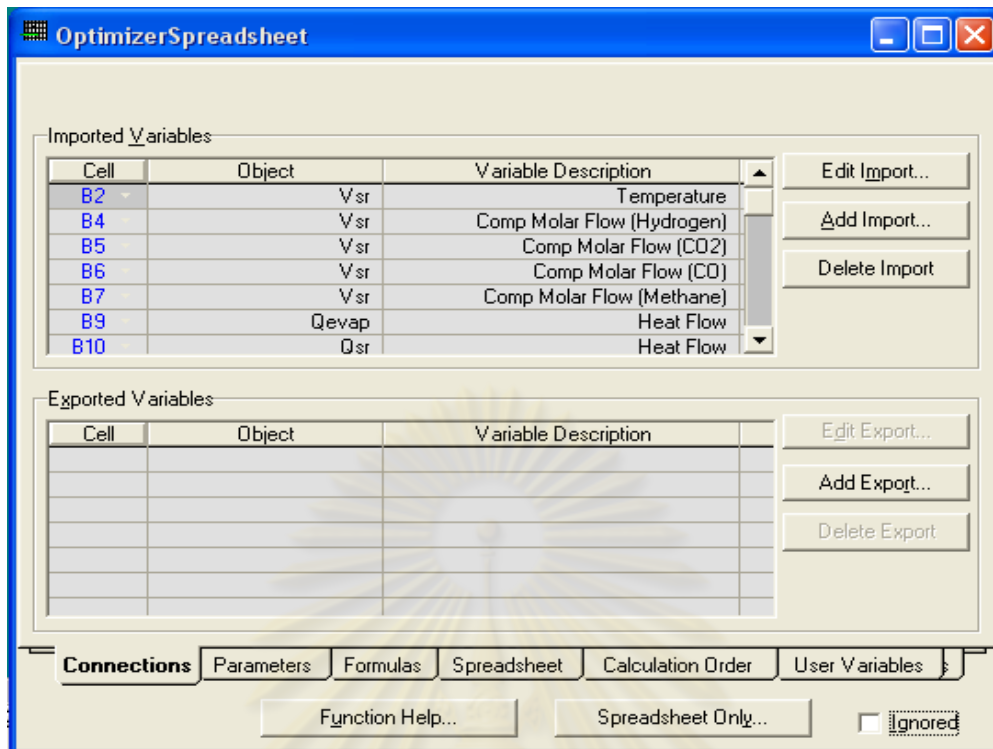
Fig. D.2 Determination of objective function

Fig. D.3 All key variables used to solve the optimization problem

Fig. D.4 shows the constraint on the outlet temperature form the reformer, which is in the range of 600 and 1200 K. After completing the input data, clicks the start bottom to run the optimize program. The results are shown in the optimization-spread sheet (Fig. D.5).
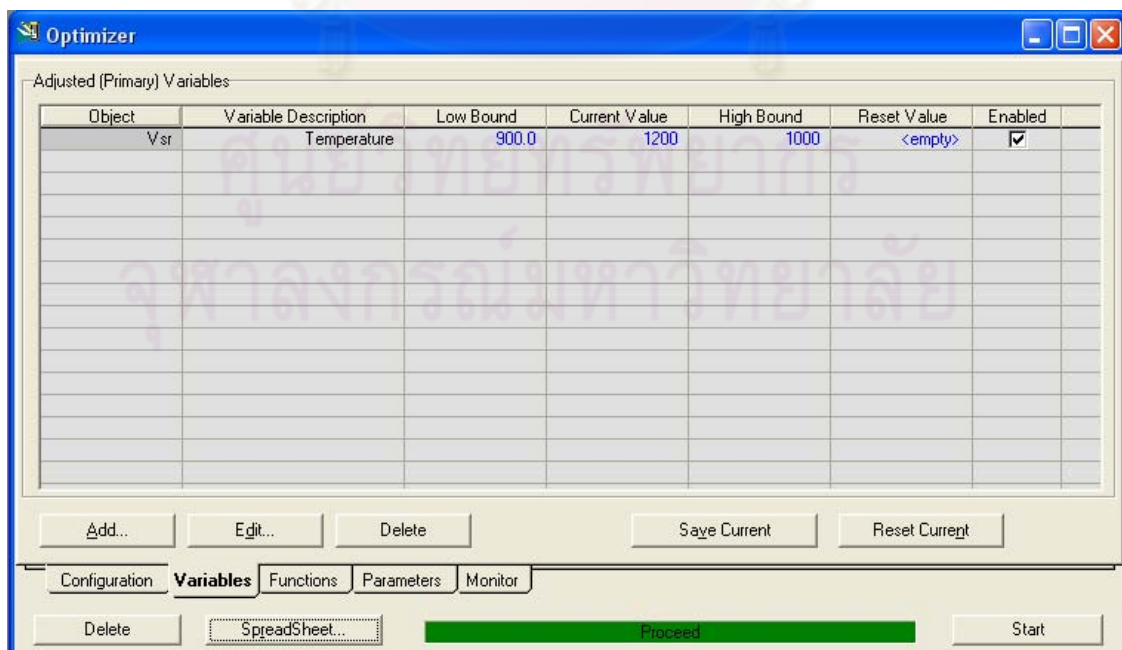

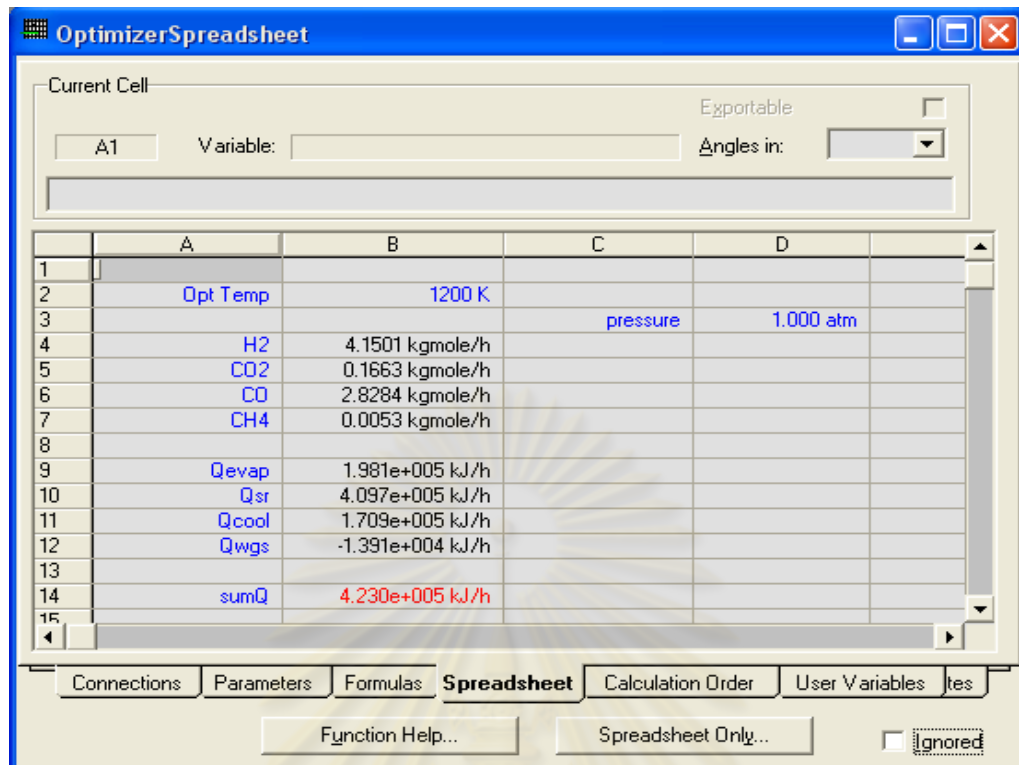**Fig. D.4** Constraint on the reformer outlet temperature

Fig. D.5 Solution of optimization problem

VITA

Miss Ghirana Jirachotdaecho was born in Bangkok on June 20, 1984. She received the Bachelor degree of Science in Chemical Technology from Department of Chemical Technology, Chulalongkorn University in 2006.